nature water

Analysis

https://doi.org/10.1038/s44221-023-00181-7

Assessing the accuracy of OpenET satellite-based evapotranspiration data to support water resource and land management applications

In the format provided by the authors and unedited

Supplementary Information for "Assessing the accuracy of OpenET satellite-based evapotranspiration data to support water resource and land management applications"

Supplementary Table 1. A list of *in situ* ET stations used in this study, including key metadata. Land cover classification and mean daily energy balance closure assignment and calculations are described in Volk et al.[1,2].

Site ID	General classification	State	Data source/network	Period of record	Energy balance	Latitude	Longitude	Elevation (m)	Land cover details	Land cover type	Measurement technique
US-A32	Grasslands	OK	AmeriFlux	06/2015-06/2017	0.90	36.8193	-97.81977	335	Hay pasture	Grasslands	Eddy covariance
US-A74	Croplands	OK	AmeriFlux	01/2016-10/2017	0.92	36.8085	-97.54885	337	Sorghum	Annual crops	Eddy covariance
US-ADR	Shrublands	NV	AmeriFlux	05/2011-05/2017	0.92	36.7653	-116.6933	842	Greasewood	Shrublands	Eddy covariance
US-AR1	Croplands	OK	AmeriFlux	06/2009-12/2012	1.09	36.4267	-99.42	611	Planted Switchgrass	Annual crops	Eddy covariance
US-ARb	Grasslands	OK	AmeriFlux	03/2005-10/2006	1.01	35.5497	-98.0402	424	Native tallgrass prairie	Grasslands	Eddy covariance
US-ARc	Grasslands	OK	AmeriFlux	03/2005-10/2006	1.02	35.5465	-98.04	424	Native tallgrass prairie (burned in March 2005)	Grasslands	Eddy covariance
US-ARM	Croplands	OK	AmeriFlux	01/2003-09/2020	0.87	36.6058	-97.4888	314	Winter wheat, corn, soy,	Annual crops	Eddy covariance
US-Aud	Grasslands	AZ	AmeriFlux	06/2002-09/2011	1.14	31.5907	-110.5104	1469	Madrean mixed grass	Grasslands	Eddy covariance
US-Bi1	Croplands	CA	AmeriFlux	08/2016-12/2019	0.78	38.0992	-121.4993	-2.7	Alfalfa	Annual crops	Eddy covariance
US-Bi2	Croplands	CA	AmeriFlux	04/2017-07/2020	0.80	38.109	-121.535	-4.98	Corn	Annual crops	Eddy covariance
US-Bkg	Croplands	SD	AmeriFlux	04/2004-03/2010	0.99	44.3453	-96.83617	510	Native grass pasture	Annual crops	Eddy covariance
US-Blk	Evergreen Forests	SD	AmeriFlux	01/2004-04/2008	0.94	44.158	-103.65	1718	Ponderosa pine	Evergreen Forests	Eddy covariance
US-Blo	Evergreen Forests	CA	AmeriFlux	06/1997-10/2007	0.93	38.8953	-120.6328	1315	Ponderosa pine plantation, mixed-	Evergreen Forests	Eddy covariance
US-Bo1	Croplands	IL	AmeriFlux	08/1996-04/2008	0.84	40.0062	-88.2904	219	Corn (2005, 2007) and soy rotation (2006, 2008), no-	Annual crops	Eddy covariance
US-Br1	Croplands	IA	AmeriFlux	04/2005-11/2011	0.81	41.9749	-93.6906	313	Corn and soy rotation	Annual crops	Eddy covariance
US-Br3	Croplands	IA	AmeriFlux	01/2005-11/2011	0.81	41.9747	-93.69357	313	Corn and soy rotation	Annual crops	Eddy covariance
US-Ced	Shrublands	NJ	AmeriFlux	07/2005-12/2014	1.08	39.8379	-74.3791	58	Pitch pine prescribed	Shrublands	Eddy covariance
US-CMW	Wetland/Riparian	AZ	AmeriFlux	03/2001-12/2019	0.87	31.6637	-110.1777	1199	Riparian mesquite	Riparian	Eddy covariance
US-CRT	Croplands	OH	AmeriFlux	01/2011-12/2013	0.77	41.6285	-83.34709	180	Soy and winter wheat, no	Annual crops	Eddy covariance
US-Ctn	Grasslands	SD	AmeriFlux	11/2006-09/2009	0.71	43.95	-101.8466	744	Grasslands	Grasslands	Eddy covariance
US-CZ3	Evergreen Forests	CA	AmeriFlux	07/2011-10/2016	1.21	37.0674	-119.1951	2015	Pine/fir forest	Evergreen Forests	Eddy covariance
US-Dix	Mixed Forests	NJ	AmeriFlux	04/2005-04/2008	1.06	39.9712	-74.43455	48	Oak/pine forest	Mixed Forests	Eddy covariance
US-Dk1	Croplands	NC	AmeriFlux	01/2006-11/2008	0.87	35.9712	-79.09338	168	Grass (Festuca	Annual crops	Eddy covariance
US-Dk2	Mixed Forests	NC	AmeriFlux	07/2006-04/2008	0.89	35.9736	-79.10043	168	Mature oak-hickory forest	Mixed Forests	Eddy covariance
US-Esm	Wetland/Riparian	FL	AmeriFlux	01/2008-11/2013	0.80	25.4379	-80.5946	1.07	Everglades peat and marl forming wetlands	Wetlands	Eddy covariance
US-Fmf	Evergreen Forests	AZ	AmeriFlux	08/2005-12/2010	0.83	35.1426	-111.7273	2160	Ponderosa pine forest	Evergreen Forests	Eddy covariance
US-FPe	Grasslands	MT	AmeriFlux	01/2000-06/2008	1.07	48.3077	-105.1019	634	Grassland	Grasslands	Eddy covariance
US-FR2	Mixed Forests	TX	AmeriFlux	01/2005-12/2007	0.78	29.9495	-97.99623	271.9	Mesquite Juniper forest	Mixed Forests	Eddy covariance
US-Fuf	Evergreen Forests	AZ	AmeriFlux	09/2005-12/2010	0.96	35.089	-111.762	2180	Ponderosa pine forest,	Evergreen Forests	Eddy covariance
US-Fwf	Grasslands	AZ	AmeriFlux	06/2005-12/2010	0.97	35.4454	-111.7718	2270	Grassland, after severe fire removed ponderosa	Grasslands	Eddy covariance
US-GLE	Evergreen Forests	WY	AmeriFlux	01/1999-03/2018	0.73	41.3665	-106.2399	3197	85% Engelmann spruce 15% Subalpine fir	Evergreen Forests	Eddy covariance
US-GMF	Mixed Forests	CT	AmeriFlux	05/1999-01/2002	0.87	41.9667	-73.23333	380	Hemlock, pine, with mixed deciduous forest	Mixed Forests	Eddy covariance
US-Goo	Grasslands	MS	AmeriFlux	05/2002-11/2006	0.83	34.2547	-89.8735	87	Grassland	Grasslands	Eddy covariance
US-Hn2	Grasslands	WA	AmeriFlux	01/2016-12/2018	0.85	46.6889	-119.4641	117.5	Cheatgrass and Russian	Grasslands	Eddy covariance
US-Hn3	Shrublands	WA	AmeriFlux	11/2017-12/2018	0.87	46.6878	-119.4615	120.9	Cheatgrass, Russian thistle, bitterbrush, sagebrush, and	Shrublands	Eddy covariance
US-IB1	Croplands	IL	AmeriFlux	07/2005-12/2018	0.79	41.8593	-88.22273	226.5	Corn and soybean rotation	Annual crops	Eddy covariance
US-IB2	Grasslands	IL	AmeriFlux	10/2004-12/2018	0.78	41.8406	-88.24103	226.5	Restored prairie	Grasslands	Eddy covariance
US-Jo2	Shrublands	NM	AmeriFlux	08/2010-12/2019	0.80	32.5849	-106.6032	1469	Open phreatophyte	Shrublands	Eddy covariance
US-KLS	Croplands	KS	AmeriFlux	12/2014-12/2016	0.78	38.7745	-97.5684	373	Wheatgrass	Annual crops	Eddy covariance
US-KM4	Grasslands	MI	AmeriFlux	07/2010-12/2018	0.78	42.4423	-85.33006	288	Smooth brome grass	Grasslands	Eddy covariance
US-KS2	Shrublands	FL	AmeriFlux	04/2000-09/2006	0.81	28.6086	-80.6715	3	Scrub oak, fire in 1996	Shrublands	Eddy covariance
US-LS1	Grasslands	AZ	AmeriFlux	03/2003-12/2007	0.76	31.5615	-110.1403	1230	Bunchgrass	Grasslands	Eddy covariance
US-Me1	Evergreen Forests	OR	AmeriFlux	06/2004-05/2005	0.98	44.5794	-121.5	896	Ponderosa pine forest, burn replaced stand in	Evergreen Forests	Eddy covariance
US-Me2	Evergreen Forests	OR	AmeriFlux	01/2002-07/2020	0.93	44.4523	-121.5574	1253	Mature ponderosa pine	Evergreen Forests	Eddy covariance
US-Me5	Evergreen Forests	OR	AmeriFlux	01/2000-12/2002	0.76	44.4372	-121.5668	1188	Ponderosa pine forest,	Evergreen Forests	Eddy covariance
US-Me6	Evergreen Forests	OR	AmeriFlux	10/2014-07/2020	0.83	44.3233	-121.6078	998	Ponderosa pine forest,	Evergreen Forests	Eddy covariance
US-Mj1	Croplands	MT	AmeriFlux	04/2013-09/2014	0.94	46.9948	-109.6138	1285	Wheat	Annual crops	Eddy covariance
US-Mj2	Croplands	MT	AmeriFlux	04/2014-09/2014	1.03	46.9957	-109.6295	1277	Summer fallow	Annual crops	Eddy covariance
US-MMS	Mixed Forests	IN	AmeriFlux	01/1999-12/2014	0.76	39.3232	-86.4131	275	Mature broadleaf forest, maple. beech, oak, hickory	Mixed Forests	Eddy covariance
US-MOz	Mixed Forests	MO	AmeriFlux	05/2006-12/2017	0.76	38.7441	-92.2	219.4	Oak/hickory/pine closed forest	Mixed Forests	Eddy covariance
US-NC2	Evergreen Forests	NC	AmeriFlux	01/2005-12/2019	1.09	35.803	-76.6685	5	Loblolly pine plantation	Evergreen Forests	Eddy covariance
US-NC3	Evergreen Forests	NC	AmeriFlux	03/2013-11/2019	1.07	35.799	-76.656	5	Loblolly pine forest, planted after clearcut in 2012	Evergreen Forests	Eddy covariance

Site ID	General classification	State	Data source/network	Period of record	Energy balance	Latitude	Longitude	Elevation (m)	Land cover details	Land cover type	Measurement technique
US-NC4	Wetland/Riparian	NC	AmeriFlux	02/2009-12/2019	1.10	35.7879	-75.9038	1	Forested wetland	Wetlands	Eddy covariance
US-Ne1	Croplands	NE	AmeriFlux	06/2001-12/2014	0.79	41.1651	-96.47664	361	Agriculture (continuous maize)	Annual crops	Eddy covariance
US-Ne2	Croplands	NE	AmeriFlux	06/2001-12/2014	0.83	41.1649	-96.4701	362	Agriculture (maize-soybean rotation)	Annual crops	Eddy covariance
US-Ne3	Croplands	NE	AmeriFlux	06/2001-12/2014	0.87	41.1797	-96.43965	363	Agriculture (maize-soybean rotation)	Annual crops	Eddy covariance
US-NR1	Evergreen Forests	CO	AmeriFlux	06/1999-12/2019	0.81	40.0329	-105.5464	3050	Subalpine fir, Engelmann spruce, and lodgepole pine	Evergreen Forests	Eddy covariance
US-Oho	Mixed Forests	OH	AmeriFlux	01/2004-12/2013	0.82	41.5545	-83.8438	230	Oak woodlands	Mixed Forests	Eddy covariance
US-Ro1	Croplands	MN	AmeriFlux	01/2011-12/2016	0.78	44.7143	-93.0898	260	Agricultural, corn and soybean rotation	Annual crops	Eddy covariance
US-Ro2	Croplands	MN	AmeriFlux	01/2016-12/2016	0.76	44.7288	-93.0888	292	Corn-Soybean-Kura Clover annual rotation	Annual crops	Eddy covariance
US-Ro3	Croplands	MN	AmeriFlux	07/2004-12/2007	0.86	44.7217	-93.0893	260	Corn-Soybean annual rotation (corn: 2003, 2005, 2007, 2009, 2011, 2013 soybean: 2004, 2006, 2008, 2010, 2012, 2014)	Annual crops	Eddy covariance
US-Ro4	Grasslands	MN	AmeriFlux	09/2015-06/2020	0.83	44.6781	-93.0723	274	Restored prarie, Andropogon gerardii, Sorghastrum nutans, and Elymus canadensis	Grasslands	Eddy covariance
US-Ro5	Croplands	MN	AmeriFlux	03/2017-12/2017	0.77	44.691	-93.0576	283	Corn/soy rotation	Annual crops	Eddy covariance
US-Ro6	Croplands	MN	AmeriFlux	03/2017-12/2017	0.80	44.6946	-93.05776	282	Corn/soybean/clover rotation	Annual crops	Eddy covariance
US-Rwe	Shrublands	ID	AmeriFlux	01/2003-09/2007	0.93	43.0653	-116.7591	2098	Mixed sagebrush	Shrublands	Eddy covariance
US-Rwf	Shrublands	ID	AmeriFlux	06/2014-01/2018	0.85	43.1207	-116.7231	1878	Sagebrush, prescribed fire in 2007	Shrublands	Eddy covariance
US-Rws	Shrublands	ID	AmeriFlux	09/2014-09/2018	0.87	43.1675	-116.7132	1425	The site is a grazing alotment with light cattle grazing in spring.	Shrublands	Eddy covariance
US-SCg	Grasslands	CA	AmeriFlux	08/2008-04/2011	0.89	33.7365	-117.6946	465	Grassland	Grasslands	Eddy covariance
US-SCs	Shrublands	CA	AmeriFlux	08/2008-10/2014	0.81	33.7343	-117.696	470	Coastal sage scrub	Shrublands	Eddy covariance
US-SCw	Shrublands	CA	AmeriFlux	09/2008-12/2009	0.88	33.6047	-116.4527	1281	Pinyon/Juniper woodland	Shrublands	Eddy covariance
US-SdH	Grasslands	NE	AmeriFlux	05/2004-12/2009	1.04	42.0693	-101.4072	1081	Grass pasture	Grasslands	Eddy covariance
US-Skr	Wetland/Riparian	FL	AmeriFlux	01/2004-08/2011	0.93	25.3629	-81.07758	0	This is a tall (up to 20 m) mangrove forest.	Wetlands	Eddy covariance
US-Slt	Mixed Forests	NJ	AmeriFlux	01/2005-12/2014	1.08	39.9138	-74.596	30	Oak forest	Mixed Forests	Eddy covariance
US-Sne	Wetland/Riparian	CA	AmeriFlux	05/2016-12/2019	0.85	38.0369	-121.7547	-5	Restored wetland	Wetlands	Eddy covariance
US-SO2	Shrublands	CA	AmeriFlux	03/1997-12/2006	0.99	33.3738	-116.6228	1394	Chaparral, severe fire in 2003	Shrublands	Eddy covariance
US-SO3	Shrublands	CA	AmeriFlux	03/1997-12/2006	0.90	33.3771	-116.6226	1429	Chaparral, severe fire in 2003	Shrublands	Eddy covariance
US-SO4	Shrublands	CA	AmeriFlux	01/2004-12/2006	0.87	33.3845	-116.6406	1429	Old-growth chaparral ecosystem	Shrublands	Eddy covariance
US-SP2	Evergreen Forests	FL	AmeriFlux	02/1999-07/2008	0.89	29.7648	-82.24482	50	Slash pine (Pinus elliottii) plantation, planted in Jan. 1999	Evergreen Forests	Eddy covariance
US-SP3	Evergreen Forests	FL	AmeriFlux	01/1999-12/2010	0.85	29.7548	-82.16328	50	Even aged high density slash pine (Pinus elliottii) plantation.	Evergreen Forests	Eddy covariance
US-SRC	Mixed Forests	AZ	AmeriFlux	03/2008-06/2014	0.82	31.9083	-110.8395	950	Greasewood	Mixed Forests	Eddy covariance
US-SRG	Grasslands	AZ	AmeriFlux	04/2008-06/2020	0.91	31.7894	-110.8277	1291	C4 grassland pasture	Grasslands	Eddy covariance
US-SRM	Shrublands	AZ	AmeriFlux	01/2004-06/2020	0.89	31.8214	-110.8661	1120	MODIS website lists this as Open Shrublands (OSO), but site is a Desert Grassland that has been fully encroached by Mesquite (now about 35% canopy cover, mean canopy height > 2 m)	Shrublands	Eddy covariance
US-Srr	Wetland/Riparian	CA	AmeriFlux	03/2016-10/2017	0.86	38.2006	-122.0264	8	Brackish tidal marsh	Wetlands	Eddy covariance
US-SRS	Shrublands	AZ	AmeriFlux	05/2011-11/2018	0.94	31.8173	-110.8508	1169	Mesquite savanna, herbicide applied in 2016	Shrublands	Eddy covariance
US-Tw2	Croplands	CA	AmeriFlux	05/2012-04/2013	0.77	38.1047	-121.6433	-5	Corn on peat soil	Annual crops	Eddy covariance
US-Tw3	Croplands	CA	AmeriFlux	05/2013-06/2018	0.85	38.1159	-121.6467	-9	Alfalfa	Annual crops	Eddy covariance
US-Twt	Croplands	CA	AmeriFlux	04/2009-04/2017	0.90	38.1087	-121.6531	-7	Rice	Annual crops	Eddy covariance
US-Var	Grasslands	CA	AmeriFlux	10/2000-08/2020	0.94	38.4133	-120.9507	129	Annual grasses and forbs	Grasslands	Eddy covariance
US-WBW	Mixed Forests	TN	AmeriFlux	01/1995-06/2007	0.75	35.9588	-84.28743	283	Oak/hickory broadleaf forest	Mixed Forests	Eddy covariance
US-WCr	Mixed Forests	WI	AmeriFlux	02/1999-04/2020	0.89	45.8059	-90.0799	520	sugar maple (Acer saccharum), basswood (Tilia americana), and yellow birch (Betula alleghaniensis).	Mixed Forests	Eddy covariance
US-Wkg	Grasslands	AZ	AmeriFlux	05/2004-06/2020	0.93	31.7365	-109.9419	1531	Desert grassland	Grasslands	Eddy covariance
US-xAE	Grasslands	OK	AmeriFlux	02/2018-05/2020	0.76	35.4106	-99.05879	516	Grass pasture	Grasslands	Eddy covariance
US-xDC	Grasslands	ND	AmeriFlux	10/2017-05/2020	0.74	47.1617	-99.10656	559	Prairie grasslands, mid- to tall-height	Grasslands	Eddy covariance
US-xDL	Mixed Forests	AL	AmeriFlux	01/2017-05/2020	0.83	32.5417	-87.80389	22	Oak and hickory	Mixed Forests	Eddy covariance
US-xDS	Grasslands	FL	AmeriFlux	01/2018-05/2020	0.75	28.125	-81.4362	15	Native grasses and wetlands	Grasslands	Eddy covariance

Site ID	General classification	State	Data source/network	Period of record	Energy balance	Latitude	Longitude	Elevation (m)	Land cover details	Land cover type	Measurement technique
US-xNG	Grasslands	ND	AmeriFlux	10/2017-04/2020	0.71	46.7697	-100.9154	578	Smooth Brome and Kentucky blue grass grassland	Grasslands	Eddy covariance
US-xRM	Evergreen Forests	CO	AmeriFlux	06/2017-05/2020	0.65	40.2759	-105.5459	2743	Ponderosa pine, open canopy	Evergreen Forests	Eddy covariance
US-xSB	Evergreen Forests	FL	AmeriFlux	12/2017-05/2020	0.82	29.6893	-81.99343	45	Pine forest, longleaf and loblolly	Evergreen Forests	Eddy covariance
US-xSL	Croplands	CO	AmeriFlux	06/2017-05/2020	0.78	40.4619	-103.0293	1364	Winter wheat, millet, and maize, no-till	Annual crops	Eddy covariance
US-xST	Mixed Forests	WI	AmeriFlux	08/2018-05/2020	0.77	45.5089	-89.58637	481	Early successional, even-aged aspen stand, with some red maple and balsam fir	Mixed Forests	Eddy covariance
US-xUN	Mixed Forests	MI	AmeriFlux	08/2017-05/2020	0.74	46.2339	-89.53725	518	Maple, aspen, birch mesic forest	Mixed Forests	Eddy covariance
MB_Pch	Croplands	CA	CSUMB	04/2012-12/2015	1.00	36.4587	-119.5801	90	Peach	Orchards	Eddy covariance
Ellendale	Croplands	LA	Delta-Flux	8/2018-12/2020	0.77	29.6333	-90.82766	2	Sugarcane	Annual crops	Eddy covariance
manilacotton	Croplands	AR	Delta-Flux	5/2016-10/2018	0.80	35.8872	-90.1371	73	Cotton	Annual crops	Eddy covariance
stonevillesoy	Croplands	MS	Delta-Flux	04/2017-07/2019	0.81	33.4433	-90.8865	37	Soy	Annual crops	Eddy covariance
US-OF1	Croplands	AR	Delta-Flux	5/2017-9/2017	0.84	35.7371	-90.0492	70	Rice	Annual crops	Eddy covariance
US-OF2	Croplands	AR	Delta-Flux	6/2017-9/2017	0.76	35.7406	-90.0489	70	Rice	Annual crops	Eddy covariance
US-OF4	Croplands	AR	Delta-Flux	5/2018-8/2018	0.89	35.7343	-90.03798	71	Rice	Annual crops	Eddy covariance
US-OF6	Croplands	AR	Delta-Flux	5/2018-8/2018	0.78	35.73	-90.04033	70	Rice	Annual crops	Eddy covariance
S2	Croplands	OR	DRI	09/2017-04/2021	0.80	43.4171	-118.6142	1255	Alfalfa	Annual crops	Eddy covariance
ALARC2_Smith6	Croplands	AZ	USDA-ARS	01/2018-06/2018	0.84	32.6973	-114.5154	45	Wheat	Annual crops	Eddy covariance
Almond_High	Croplands	CA	USDA-ARS	10/2016-10/2019	0.83	36.1697	-120.201	147	Almond	Orchards	Eddy covariance
Almond_Low	Croplands	CA	USDA-ARS	10/2016-10/2019	0.84	36.9466	-120.1024	78	Almond	Orchards	Eddy covariance
Almond_Med	Croplands	CA	USDA-ARS	09/2016-10/2019	0.82	36.1777	-120.2026	147	Almond	Orchards	Eddy covariance
JPL1_JV114	Croplands	AZ	USDA-ARS	09/2018-12/2018	0.77	32.6563	-114.6565	35	Iceberg	Vegetable crops	Eddy covariance
JPL1_Smith5	Croplands	AZ	USDA-ARS	12/2017-06/2018	0.78	32.6975	-114.5195	44	Wheat	Annual crops	Eddy covariance
UA1_HartFarm	Croplands	AZ	USDA-ARS	12/2018-05/2019	0.92	33.0774	-112.1121	355	Wheat	Annual crops	Eddy covariance
UA1_JV187	Croplands	AZ	USDA-ARS	03/2018-07/2018	0.87	32.7065	-114.7085	36	Sudan	Annual crops	Eddy covariance
UA1_KN18	Croplands	AZ	USDA-ARS	09/2018-11/2018	0.94	32.7762	-114.5888	40	Cauliflower	Vegetable crops	Eddy covariance
UA2_JV330	Croplands	AZ	USDA-ARS	11/2018-01/2019	0.89	32.7122	-114.5742	40	Spring mix	Vegetable crops	Eddy covariance
UA2_KN20	Croplands	AZ	USDA-ARS	02/2019-03/2019	0.87	32.7795	-114.5811	40	Baby Leaf Lettuce	Vegetable crops	Eddy covariance
UA3_JV108	Croplands	AZ	USDA-ARS	03/2018-06/2018	0.87	32.7207	-114.706	37	Sudan	Annual crops	Eddy covariance
UA3_KN15	Croplands	AZ	USDA-ARS	09/2018-11/2018	0.88	32.7802	-114.5883	39	Broccoli	Vegetable crops	Eddy covariance
LYS_NE	Croplands	TX	USDA-ARS	5/2013-10/2016		35.1881	-102.0955	1173	Corn and sorghum, subsurface drip irrigation	Annual crops	Weighing lysimete
LYS_NW	Croplands	TX	USDA-ARS	6/2013-10/2016		35.1881	-102.0979	1174	Corn and sorghum, mid elevation sprinkler application	Annual crops	Weighing lysimete
LYS_SE	Croplands	TX	USDA-ARS	5/2013-10/2016		35.1861	-102.0956	1172	Corn and sorghum, subsurface drip irrigation	Annual crops	Weighing lysimete
LYS_SW	Croplands	TX	USDA-ARS	6/2013-10/2016		35.1861	-102.0979	1174	Corn and sorghum, mid elevation sprinkler application	Annual crops	Weighing lysimete
BAR012	Croplands	CA	USDA-ARS GRAPEX	05/2017-11/2018	0.85	38.751	-122.975	102	Vineyard	Vineyards	Eddy covariance
RIP760	Croplands	CA	USDA-ARS GRAPEX	05/2017-11/2018	0.88	36.839	-120.21	57	Vineyard	Vineyards	Eddy covariance
SLM001	Croplands	CA	USDA-ARS GRAPEX	01/2017-11/2018	0.94	38.289	-121.118	39	Vineyard	Vineyards	Eddy covariance
B_01	Croplands	NV	USGS NWSC	03/2005-04/2007		39.055	-119.134	1326	Non Irrigated Alfalfa	Annual crops	Bowen Ratio
B_11	Croplands	NV	USGS NWSC	03/2005-03/2007		39.108	-119.146	1317	Irrigated Alfalfa	Annual crops	Bowen Ratio
ET_1	Shrublands	NV	USGS NWSC	01/2004-10/2004		39.029	-119.808	1420	Greasewood/Rabbitbrush	Shrublands	Bowen Ratio
ET_8	Croplands	NV	USGS NWSC	06/2003-11/2004		38.859	-119.764	1471	Irrigated Pasture Grass	Annual crops	Bowen Ratio
MR	Wetland/Riparian	NV	USGS NWSC	07/2003-09/2006		36.691	-114.688	503	Mesquite	Riparian	Bowen Ratio
TAM	Wetland/Riparian	NV	USGS NWSC	03/2005-03/2007		38.851	-118.773	1222	Salt Cedar	Riparian	Bowen Ratio
VR	Wetland/Riparian	NV	USGS NWSC	02/2003-03/2005		36.588	-114.328	370	Salt Cedar	Riparian	Bowen Ratio
AFD	Shrublands	NV	USGS NWSC	11/2011-11/2013	0.83	36.4909	-116.2533	709	Shadscale	Shrublands	Eddy covariance
AFS	Grasslands	NV	USGS NWSC	11/2011-11/2013	0.99	36.4926	-116.2594	708	Salt Grass	Grasslands	Eddy covariance
BPHV	Grasslands	CA	USGS NWSC	10/2012-09/2013	0.77	38.2097	-119.2914	1997	Pasture Grass	Grasslands	Eddy covariance
BPLV	Grasslands	CA	USGS NWSC	10/2012-09/2013	0.98	38.2267	-119.2861	2023	Pasture grass	Grasslands	Eddy covariance
DVDV	Shrublands	NV	USGS NWSC	10/2009-09/2011	0.77	39.7625	-117.9601	1046	Greasewood/Big Saltbush/Seepweed	Shrublands	Eddy covariance
KV_1	Shrublands	NV	USGS NWSC	08/2011-08/2012	0.89	39.5371	-116.3576	1859	Greasewood/Rabbitbrush	Shrublands	Eddy covariance
KV_2	Shrublands	NV	USGS NWSC	08/2010-08/2012	0.91	39.6197	-116.2134	1845	Greasewood/Rabbitbrush/Salt Grass	Shrublands	Eddy covariance
KV_4	Grasslands	NV	USGS NWSC	11/2011-11/2012	0.90	39.5987	-116.1642	1833	Meadow Grass	Grasslands	Eddy covariance
SPV_1	Shrublands	NV	USGS NWSC	09/2005-08/2007	0.81	38.7776	-114.4678	1763	Greasewood/Rabbitbrush	Shrublands	Eddy covariance
SPV_3	Grasslands	NV	USGS NWSC	09/2005-08/2007	0.93	38.9367	-114.4212	1763	Mixed Grasses	Grasslands	Eddy covariance
SV_5	Shrublands	NV	USGS NWSC	10/2007-09/2009	0.95	39.0325	-114.4855	1760	Greasewood/Rabbitbrush	Shrublands	Eddy covariance
SV_6	Shrublands	NV	USGS NWSC	10/2007-09/2009	0.95	39.0429	-114.4831	1756	Greasewood/Rabbitbrush	Shrublands	Eddy covariance
UMVW	Shrublands	NV	USGS NWSC	10/2005-09/2006	1.06	37.5204	-114.5832	1250	Rabbitbrush	Shrublands	Eddy covariance
WRV_1	Shrublands	NV	USGS NWSC	09/2005-08/2007	0.99	38.4136	-115.0509	1600	Greasewood	Shrublands	Eddy covariance
WRV_2	Shrublands	NV	USGS NWSC	09/2006-08/2007	0.82	38.6405	-115.1026	1622	Greasewood	Shrublands	Eddy covariance

Site ID	DOI/link	Team member	Member role	Member institution	Member email	Site name
US-A32	10.17190/AMF/1436327	Lara Kueppers	PI	Lawrence Berkeley National Laboratory	lmkueppers@lbl.gov	ARM-SGP Medford hay pasture
US-A74	10.17190/AMF/1436328	Lara Kueppers	PI	Lawrence Berkeley National Laboratory	lmkueppers@lbl.gov	ARM SGP milo field
US-ADR	10.17190/AMF/1418680	Michael Moreo	PI	U.S. Geological Survey	mtmoreo@usgs.gov	Amargosa Desert Research Site (ADRS)
US-AR1	10.17190/AMF/1246137	Dave Billesbach	PI	University of Nebraska	dbillesbach1@unl.edu	ARM USDA UNL OSU Woodward Switchgrass 1
US-ARb	10.17190/AMF/1246025	Margaret Torn	PI	Lawrence Berkeley National Laboratory	mstorn@lbl.gov	ARM Southern Great Plains burn site- Lamont
US-ARc	10.17190/AMF/1246026	Margaret Torn	PI	Lawrence Berkeley National Laboratory	mstorn@lbl.gov	ARM Southern Great Plains control site- Lamont
US-ARM	10.17190/AMF/1246027	Sebastien Biraud	PI	Lawrence Berkeley National Laboratory	SCBiraud@lbl.gov	ARM Southern Great Plains site- Lamont
US-Aud	10.17190/AMF/1246028	Tilden Meyers	PI	NOAA/ARL	Tilden.Meyers@noaa.gov	Audubon Research Ranch
US-Bi1	10.17190/AMF/1480317	Dennis Baldocchi	PI	University of California, Berkeley	Baldocchi@berkeley.edu	Bouldin Island Alfalfa
US-Bi2	10.17190/AMF/1419513	Dennis Baldocchi	PI	University of California, Berkeley	baldocchi@berkeley.edu	Bouldin Island corn
US-Bkg	10.17190/AMF/1246040	Tilden Meyers	PI	NOAA/ARL	Tilden.Meyers@noaa.gov	Brookings
US-Blk	10.17190/AMF/1246031	Tilden Meyers	PI	NOAA/ARL	Tilden.Meyers@noaa.gov	Black Hills
US-Blo	10.17190/AMF/1246032	Allen Goldstein	PI	University of California, Berkeley	ahg@berkeley.edu	Blodgett Forest
US-Bo1	10.17190/AMF/1246036	Tilden Meyers	PI	NOAA/ARL	Tilden.Meyers@noaa.gov	Bondville
US-Br1	10.17190/AMF/1246038	John Prueger	PI	National Laboratory for Agriculture and the Environment	john.prueger@ars.usda.gov	Brooks Field Site 10- Ames
US-Br3	10.17190/AMF/1246039	John Prueger	PI	National Laboratory for Agriculture and the Environment	john.prueger@ars.usda.gov	Brooks Field Site 11- Ames
US-Ced	10.17190/AMF/1246043	Ken Clark	PI	USDA Forest Service	kennethclark@fs.fed.us	Cedar Bridge
US-CMW	10.17190/AMF/1660339	Russell Scott	PI	USDA-ARS	russ.scott@ars.usda.gov	Charleston Mesquite Woodland
US-CRT	10.17190/AMF/1246156	Jiquan Chen	PI	University of Toledo / Michigan State University	jqchen@msu.edu	Curtice Walter-Berger cropland
US-Ctn	10.17190/AMF/1246117	Tilden Meyers	PI	NOAA/ARL	tilden.meyers@noaa.gov	Cottonwood
US-CZ3	10.17190/AMF/1419512	Michael Goulden	PI	UC Irvine	mgoulden@uci.edu	Sierra Critical Zone, Sierra Transect, Sierran Mixed Conifer, P301
US-Dix	10.17190/AMF/1246045	Ken Clark	PI	USDA Forest Service	kennethclark@fs.fed.us	Fort Dix
US-Dk1	10.17190/AMF/1246046	Chris Oishi	PI	USDA Forest Service	christopher.oishi@gmail.com	Duke Forest-open field
US-Dk2	10.17190/AMF/1246047	A. Christopher Oishi	PI	USDA Forest Service	acoishi@fs.fed.us	Duke Forest-hardwoods
US-Esm	10.17190/AMF/1246119	Gregory Starr	PI	University of Alabama	gstarr@bama.ua.edu	Everglades (short hydroperiod marsh)
US-Fmf	10.17190/AMF/1246050	Sabina Dore	PI	Northern Arizona University	Sabina.Dore@nau.edu	Flagstaff - Managed Forest
US-FPe	10.17190/AMF/1246053	Tilden Meyers	PI	NOAA/ARL	Tilden.Meyers@noaa.gov	Fort Peck
US-FR2	10.17190/AMF/1246054	Marcy Litvak	PI	University of New Mexico	mlitvak@unm.edu	Freeman Ranch- Mesquite Juniper
US-Fuf	10.17190/AMF/1246051	Sabina Dore	PI	Northern Arizona University	Sabina.Dore@nau.edu	Flagstaff - Unmanaged Forest
US-Fwf	10.17190/AMF/1246052	Sabina Dore	PI	Northern Arizona University	Sabina.Dore@nau.edu	Flagstaff - Wildfire
US-GLE	10.17190/AMF/1246056	Bill Massman	PI	USDA Forest Service	wmassman@fs.fed.us	GLEES
US-GMF	10.17190/AMF/1246057	Xuhui Lee	PI	Yale University	xuhui.lee@yale.edu	Great Mountain Forest
US-Goo	10.17190/AMF/1246058	Tilden Meyers	PI	NOAA/ARL	Tilden.Meyers@noaa.gov	Goodwin Creek
US-Hn2	10.17190/AMF/1562389	Heping Liu	PI	Washington State University	heping.liu@wsu.edu	Hanford 100H grassland
US-Hn3	10.17190/AMF/1543379	Heping Liu	PI	Washington State University	heping.liu@wsu.edu	Hanford 100H sagebrush
US-IB1	10.17190/AMF/1246065	Roser Matamala	PI	Argonne National Laboratory	matamala@anl.gov	Fermi National Accelerator Laboratory- Batavia (Agricultural site)
US-IB2	10.17190/AMF/1246066	Roser Matamala	PI	Argonne National Laboratory	matamala@anl.gov	Fermi National Accelerator Laboratory- Batavia (Prairie site)
US-Jo2	10.17190/AMF/1617696	Enrique R. Vivoni	PI	Arizona State University	vivoni@asu.edu	Jornada Experimental Range Mixed Shrubland
US-KLS	10.17190/AMF/1498745	Nathaniel Brunsell	PI	Kansas University	brunsell@ku.edu	Kansas Land Institute
US-KM4	10.17190/AMF/1634882	G. Philip Robertson	PI	Michigan State University	robert30@msu.edu	KBS Marshall Farms Smooth Brome Grass (Ref)
US-KS2	10.17190/AMF/1246070	Bert Drake	PI	Smithsonian Environmental Research Center	drakeb@si.edu	Kennedy Space Center (scrub oak)
US-LS1	10.17190/AMF/1660346	Russell Scott	PI	USDA-ARS	russ.scott@ars.usda.gov	San Pedro River Lewis Springs Sacaton Grassland
US-Me1	10.17190/AMF/1246074	Bev Law	PI	Oregon State University	bev.law@oregonstate.edu	Metolius - Eyerly burn
US-Me2	10.17190/AMF/1246076	Bev Law	PI	Oregon State University	bev.law@oregonstate.edu	Metolius mature ponderosa pine
US-Me5	10.17190/AMF/1246079	Bev Law	PI	Oregon State University	bev.law@oregonstate.edu	Metolius-first young aged pine
US-Me6	10.17190/AMF/1246128	Bev Law	PI	Oregon State University	bev.law@oregonstate.edu	Metolius Young Pine Burn

Site ID	DOI/link	Team member	Member role	Member institution	Member email	Site name
US-Mj1	10.17190/AMF/1617715	Paul C. Stoy	PI	Montana State University	paul.stoy@montana.edu	Montana Judith Basin wheat field
US-Mj2	10.17190/AMF/1617716	Paul C. Stoy	PI	Montana State University	paul.stoy@montana.edu	Montana Judith Basin summer fallow field
US-MMS	10.17190/AMF/1246080	Kim Novick	PI	Indiana University	knovick@indiana.edu	Morgan Monroe State Forest
US-MOz	10.17190/AMF/1246081	Jeffrey Wood	PI	University of Missouri	woodjd@missouri.edu	Missouri Ozark Site
US-NC2	10.17190/AMF/1246083	Asko Noormets	PI	Texas A&M University	noormets@tamu.edu	NC_Loblolly Plantation
US-NC3	10.17190/AMF/1419506	Asko Noormets	PI	Texas A&M University	noormets@tamu.edu	NC_Clearcut#3
US-NC4	10.17190/AMF/1480314	Asko Noormets	PI	Texas A&M University	noormets@tamu.edu	NC_AlligatorRiver
US-Ne1	10.17190/AMF/1246084	Andy Suyker	PI	University of Nebraska - Lincoln	asuyker1@unl.edu	Mead - irrigated continuous maize site
US-Ne2	10.17190/AMF/1246085	Andy Suyker	PI	University of Nebraska - Lincoln	asuyker1@unl.edu	Mead - irrigated maize-soybean rotation site
US-Ne3	10.17190/AMF/1246086	Andy Suyker	PI	University of Nebraska - Lincoln	asuyker1@unl.edu	Mead - rainfed maize-soybean rotation site
US-NR1	10.17190/AMF/1246088	Peter Blanken	PI	University of Colorado	Blanken@Colorado.EDU	Niwot Ridge Forest (LTER NWT1)
US-Oho	10.17190/AMF/1246089	Jiquan Chen	PI	University of Toledo / Michigan State University	jqchen@msu.edu	Oak Openings
US-Ro1	10.17190/AMF/1246092	John Baker	PI	USDA-ARS	john.baker@ars.usda.gov	Rosemount- G21
US-Ro2	10.17190/AMF/1418683	John Baker	PI	USDA-ARS	john.baker@ars.usda.gov	Rosemount- C7
US-Ro3	10.17190/AMF/1246093	John Baker	PI	USDA-ARS	John.Baker@ARS.USDA.GOV	Rosemount- G19
US-Ro4	10.17190/AMF/1419507	John Baker	PI	USDA-ARS	John.Baker@ARS.USDA.GOV	Rosemount Prairie
US-Ro5	10.17190/AMF/1419508	John Baker	PI	USDA-ARS	john.baker@ars.usda.gov	Rosemount I18_South
US-Ro6	10.17190/AMF/1419509	John Baker	PI	USDA-ARS	john.baker@ars.usda.gov	Rosemount I18_North
US-Rwe	10.17190/AMF/1617721	Gerald Flerchinger	PI	USDA Agricultural Research Service	gerald.flerchinger@ars.usda.go	RCEW Reynolds Mountain East
US-Rwf	10.17190/AMF/1617724	Gerald Flerchinger	PI	USDA Agricultural Research Service	gerald.flerchinger@ars.usda.go	RCEW Upper Sheep Prescibed Fire
US-Rws	10.17190/AMF/1375201	Gerald Flerchinger	PI	USDA Agricultural Research Service	gerald.flerchinger@ars.usda.go	Reynolds Creek Wyoming big sagebrush
US-SCg	10.17190/AMF/1419502	Mike Goulden	PI	University of California - Irvine	mgoulden@uci.edu	Southern California Climate Gradient - Grassland
US-SCs	10.17190/AMF/1419501	Mike Goulden	PI	University of California - Irvine	mgoulden@uci.edu	Southern California Climate Gradient - Coastal Sage
US-SCw	10.17190/AMF/1419504	Mike Goulden	PI	University of California - Irvine	mgoulden@uci.edu	Southern California Climate Gradient - Pinyon/Juniper Woodland
US-SdH	10.17190/AMF/1246136	Dave Billesbach	PI	University of Nebraska	dbillesbach1@unl.edu	Nebraska SandHills Dry Valley
US-Skr	10.17190/AMF/1246105	Sparkle Malone	PI	Pennsylvania State University	jdfuentes@psu.edu	Shark River Slough (Tower SRS-6) Everglades
US-Slt	10.17190/AMF/1246096	Ken Clark	PI	USDA Forest Service	kennethclark@fs.fed.us	Silas Little- New Jersey
US-Sne	10.17190/AMF/1418684	Dennis Baldocchi	PI	University of California, Berkeley	Baldocchi@berkeley.edu	Sherman Island Restored Wetland
US-SO2	10.17190/AMF/1246097	Walt Oechel	PI	San Diego State University	woechel@mail.sdsu.edu	Sky Oaks- Old Stand
US-SO3	10.17190/AMF/1246098	Walt Oechel	PI	San Diego State University	woechel@mail.sdsu.edu	Sky Oaks- Young Stand
US-SO4	10.17190/AMF/1246099	Walt Oechel	PI	San Diego State University	woechel@mail.sdsu.edu	Sky Oaks- New Stand
US-SP2	10.17190/AMF/1246101	Tim Martin	PI	University of Florida	tamartin@ufl.edu	Slashpine-Mize-clearcut-3yr,regen
US-SP3	10.17190/AMF/1246102	Tim Martin	PI	University of Florida	tamartin@ufl.edu	Slashpine-Donaldson-mid-rot- 12yrs
US-SRC	10.17190/AMF/1246127	Shirley Kurc	PI	University of Arizona	kurc@ag.arizona.edu	Santa Rita Creosote
US-SRG	10.17190/AMF/1246154	Russell Scott	PI	United States Department of Agriculture	russ.scott@ars.usda.gov	Santa Rita Grassland
US-SRM	10.17190/AMF/1246104	Russell Scott	PI	United States Department of Agriculture	russ.scott@ars.usda.gov	Santa Rita Mesquite
US-Srr	10.17190/AMF/1418685	Brian Bergamaschi	PI	USGS	bbergama@usgs.gov	Suisun marsh - Rush Ranch
US-SRS	10.17190/AMF/1660351	Enrique R. Vivoni	PI	Arizona State University	vivoni@asu.edu	Santa Rita Experimental Range Mesquite Savanna
US-Tw2	10.17190/AMF/1246148	Dennis Baldocchi	PI	University of California, Berkeley	baldocchi@berkeley.edu	Twitchell Corn
US-Tw3	10.17190/AMF/1246149	Dennis Baldocchi	PI	University of California, Berkeley	baldocchi@berkeley.edu	Twitchell Alfalfa
US-Twt	10.17190/AMF/1246140	Dennis Baldocchi	PI	University of California, Berkeley	baldocchi@berkeley.edu	Twitchell Island
US-Var	10.17190/AMF/1245984	Dennis Baldocchi	PI	University of California, Berkeley	Baldocchi@berkeley.edu	Vaira Ranch- Ione
US-WBW	10.17190/AMF/1246109	Tilden Meyers	PI	NOAA/ARL	Tilden.Meyers@noaa.gov	Walker Branch Watershed
US-WCr	10.17190/AMF/1246111	Ankur Desai	PI	University of Wisconsin	desai@aos.wisc.edu	Willow Creek
US-Wkg	10.17190/AMF/1246112	Russell Scott	PI	United States Department of Agriculture	russ.scott@ars.usda.gov	Walnut Gulch Kendall Grasslands
US-xAE		Cove Sturtevant	PI	NEON	csturtevant@battelleecology.or	NEON Klemme Range Research Station (OAES)
US-xDC	10.17190/AMF/1617728	Cove Sturtevant	PI	NEON	csturtevant@battelleecology.or	NEON Dakota Coteau Field School (DCFS)
US-xDL	10.17190/AMF/1579721	Cove Sturtevant	PI	NEON	csturtevant@battelleecology.or	NEON Dead Lake (DELA)
US-xDS		Cove Sturtevant	PI	NEON	csturtevant@battelleecology.or	NEON Disney Wilderness Preserve (DSNY)

Site ID	DOI/link	Team member	Member role	Member institution	Member email	Site name
US-xNG	10.17190/AMF/1617732	Cove Sturtevant	PI	NEON	csturtevant@battelleecology.or	NEON Northern Great Plains Research Laboratory (NOGP)
US-xRM	10.17190/AMF/1579723	Cove Sturtevant	PI	NEON	csturtevant@battelleecology.or	NEON Rocky Mountain National Park, CASTNET (RMNP)
US-xSB		Cove Sturtevant	PI	NEON	csturtevant@battelleecology.or	NEON Ordway-Swisher Biological Station (OSBS)
US-xSL	10.17190/AMF/1617735	Cove Sturtevant	PI	NEON	csturtevant@battelleecology.or	NEON North Sterling, CO (STER)
US-xST	10.17190/AMF/1617737	Cove Sturtevant	PI	NEON	csturtevant@battelleecology.or	NEON Steigerwaldt Land Services (STEI)
US-xUN	10.17190/AMF/1617741	Cove Sturtevant	PI	NEON	csturtevant@battelleecology.or	NEON University of Notre Dame Environmental Research Center (UNDE)
MB_Pch		Forrest Melton			fmelton@csumb.edu	
Ellendale		Benjamin Runkle			brrunkle@uark.edu	
manilacotton		Benjamin Runkle			brrunkle@uark.edu	
stonevillesoy		Saseendran Anapalli			saseendran.anapalli@usda.gov	
US-OF1		Benjamin Runkle			brrunkle@uark.edu	
US-OF2		Benjamin Runkle			brrunkle@uark.edu	
US-OF4		Benjamin Runkle			brrunkle@uark.edu	
US-OF6		Benjamin Runkle			brrunkle@uark.edu	
S2		Richard Jasoni			Richard.Jasoni@dri.edu	
ALARC2_Smith6		Andy French			andrew.french@usda.gov	
Almond_High		Ray Anderson			ray.anderson@usda.gov	
Almond_Low		Ray Anderson			ray.anderson@usda.gov	
Almond_Med		Ray Anderson			ray.anderson@usda.gov	
JPL1_JV114		Andy French			andrew.french@usda.gov	
JPL1_Smith5		Andy French			andrew.french@usda.gov	
UA1_HartFarm		Andy French			andrew.french@usda.gov	
UA1_JV187		Andy French			andrew.french@usda.gov	
UA1_KN18		Andy French			andrew.french@usda.gov	
UA2_JV330		Andy French			andrew.french@usda.gov	
UA2_KN20		Andy French			andrew.french@usda.gov	
UA3_JV108		Andy French			andrew.french@usda.gov	
UA3_KN15		Andy French			andrew.french@usda.gov	
LYS_NE		Steven Evett			steve.evett@usda.gov	
LYS_NW		Steven Evett			steve.evett@usda.gov	
LYS_SE		Steven Evett			steve.evett@usda.gov	
LYS_SW		Steven Evett			steve.evett@usda.gov	
BAR012		William Kustas			bill.kustas@usda.gov	
RIP760		William Kustas			bill.kustas@usda.gov	
SLM001		William Kustas			bill.kustas@usda.gov	
B_01	10.3133/sir20095079	Kip Allander			kalland@usgs.gov	
B_11	10.3133/sir20095079	Kip Allander			kalland@usgs.gov	
ET_1	10.3133/sir20055288	Doug Maurer			dkmaurer@usgs.gov	
ET_8	10.3133/sir20055288	Doug Maurer			dkmaurer@usgs.gov	
MR	10.3133/sir20085116	Guy A. DeMeo			gademeo@usgs.gov	
TAM	10.3133/sir20095079	Kip Allander			kalland@usgs.gov	
VR	10.3133/sir20085116	Guy A. DeMeo			gademeo@usgs.gov	
AFD	10.5066/F7R49NZN	Michael T. Moreo			mtmoreo@usgs.gov	
AFS	10.5066/F7R49NZN	Michael T. Moreo			mtmoreo@usgs.gov	
BPHV	10.5066/F79C6WM9	Guy A. DeMeo			gademeo@usgs.gov	
BPLV	10.5066/F79C6WM9	Guy A. DeMeo			gademeo@usgs.gov	
DVDV	10.3133/pp1805	Amanda Garcia			cgarcia@usgs.gov	
KV_1	10.5066/P9NZ9XSP	Amanda Garcia			cgarcia@usgs.gov	
KV_2	10.5066/P9NZ9XSP	Amanda Garcia			cgarcia@usgs.gov	
KV_4	10.5066/P9NZ9XSP	Amanda Garcia			cgarcia@usgs.gov	
SPV_1	10.3133/sir20075078	Michael T. Moreo			mtmoreo@usgs.gov	
SPV_3	10.3133/sir20075078	Michael T. Moreo			mtmoreo@usgs.gov	
SV_5		Jay Arnone			jarnone@dri.edu	
SV_6		Jay Arnone			jarnone@dri.edu	
UMVW	10.3133/sir20085116	Guy A. DeMeo			gademeo@usgs.gov	
WRV_1	10.3133/sir20075078	Michael T. Moreo			mtmoreo@usgs.gov	
WRV_2	10.3133/sir20075078	Michael T. Moreo			mtmoreo@usgs.gov	

Supplementary Discussion 1. Discussion of energy balance closure error and uncertainty in eddy covariance data used to evaluate OpenET.

The eddy covariance (EC) technique is widely used to estimate vertical turbulent fluxes of latent energy (LE) and sensible heat (H) within a region of interest[3,4]. Other major components of the near surface energy balance (SEB) can often be estimated with additional sensors, commonly soil heat flux plates and a net radiometer to measure soil heat flux (G) and net radiation (Rn), respectively. While EC is widely used for *in situ* ET estimation and is regarded as one of the best available methods, the approach is subject to limitations that can lead to surface energy imbalance[5]. We next discuss some of the major reasons why the method often has additional data uncertainties that can result in misrepresentation of the major SEB components and give examples. We then discuss the steps taken to limit those uncertainties prior to using the EC data to evaluate OpenET remote sensing ET (RSET) data (see also Volk et al.[1,2], Melton et al.[6]).

Causes of EC closure problems may be grouped into four broad categories: instrument error, data processing error, unaccounted energy sources, and sub-mesoscale transport/secondary circulations[7]. Some error sources can be accounted for by the practitioner, including sensor calibration and maintenance, and high frequency data processing and correction methods[7]. In addition, spectral correction can also account for high-frequency spectral loss due to sensor limitations[8,9]. Many of the SEB error sources EC data are difficult to account for on a post hoc basis. These range from site land cover heterogeneity and terrain complexity, instrumentation type, placement, and micrometeorological conditions that are not well suited for the theoretical assumptions of the EC technique.

A well known source of error that is difficult to account for is sub-mesoscale eddies that are not captured by a single EC tower. This secondary circulation can appear as advection and result in under- or over-estimations of LE and H. Similarly, LE and H can be misrepresented due to other invalidations of the assumptions of the EC technique such as insufficient friction velocity to generate eddies of appropriate scale[10,11], highly stable or unstable atmospheric boundary conditions[12], or their combination[13–15]. Another well-known source of uncertainty in EC data is that Rn as measured on a tower and G from soil heat flux plates (point scales) do not correspond with the larger scale of the source area of turbulent fluxes that are temporally dynamic as a function of atmospheric circulations and land cover[16]. The scale mismatch between available energy and turbulent fluxes poses further challenges in assessing the SEB.

Other SEB closure errors in EC data may come from unaccounted energy storage, and these include heat storage in soil, air, and canopies, which can be a significant component of the SEB depending on the micrometeorological conditions and timescale[5,7]. For example, heat storage in air and biomass, as well as chemical energy stored during photosynthesis, are often overlooked as a source of SEB error in EC data[17,18] and it is often not reported with EC data or not feasible to be estimated because the required measurements are expensive, requiring additional gas and thermal probes placed along the vertical profile[19]. Soil heat storage above a soil heat flux plate can be readily measured and corrected for by using thermocouples to estimate the vertical thermal profile[20]. Plant physiology in response to micrometeorological conditions can also change the SEB; for example, in a water limited environment with plenty of available energy and warm and dry air, some plants may temporarily close their stomata to preserve water, leading to a reduction in LE and an increase in H.

Some of the sources of SEB errors (including some of those previously mentioned) may be limited by following best practices or by using post-processing techniques. For example: appropriate site placement and footprint representation[4,16], limiting instrumentation error caused by improper maintenance and calibration, e.g., cleaning dust from net radiometers can reduce error[21], and accounting for the heat storage in soil can reduce SEB error, particularly at sub-daily timescales[5,17]. Errors from instrumentation, high frequency data processing and averaging, data corrections are also important sources of uncertainty that can be accounted for by most practitioners who follow best practices, such as those set by AmeriFlux[22].

Acknowledging the inherent issues with EC data and SEB error, and that much of the decisions and steps that are needed to limit SEB error are dependent on the initial deployment of each EC system, maintenance, and processing of high-frequency data— we took further steps to limit SEB related uncertainty in the dataset used in this study. First, we gathered data from networks, such as AmeriFlux[22], which follow best practices in EC system installation, instrumentation, maintenance, and data processing. AmeriFlux provides services to help site principal investigators (PI) and technicians install EC systems, setup instrumentation and calibrate them, and perform data quality control and high frequency data processing (https://ameriflux.lbl.gov/about/ameriflux-management-project/). When gathering EC data, particularly those from other networks and university partners, we asked PIs about their site instrumentation and data quality control techniques to ensure that they were like those recommended by trusted networks. For example, we made efforts to ensure that all soil heat flux measurements were corrected for soil heat storage above heat flux plates. We also used data subject to prior quality control checks when provided. In the cases of multiple soil heat flux plate measurements, we used either the PI approved records or took the average from multiple sensors. In developing the benchmark flux dataset, we only considered flux stations where continuous measurements of all four SEB components were measured so that we could assess energy balance closure error; all of the EC stations used employed high quality instrumentation including a 3-D sonic anemometer, an open-path infrared gas analyzer, a net radiometer, and soil heat flux plates[1,2].

After the initial collection of EC data, we performed a series of quality control checks and post-processing steps, culminating with SEB closure corrections applied to turbulent fluxes[1,2].

Together these steps aimed to limit the uncertainty inherent in EC data. The first step of flux data post-processing we performed was a conservative gap-filling procedure on the half-hourly records of the SEB components using linear interpolation, where we limited the total number of gap-filled hours per day to 2 hours. This approach is more conservative than the FLUXNET2015/ONEFlux methods that use longer gap-filling windows[1,2,23]. We averaged the gap-filled SEB components to 24-hour periods, this decision was made for two reasons: (1) the OpenET models output daily ET; and (2) to limit the error caused by diurnal phase shifts in heat storage (in soil, air, and biomass), available energy, and turbulent fluxes that may result in SEB error that are higher at shorter timescales. We acknowledge that 24-hour averaging will not remove all sources of SEB error, such as energy use by photosynthesis or storage of energy in dense canopies, however it will limit some of the error. For example, soil heat storage will often have a strong diurnal pattern, going up during the morning and releasing heat as longwave radiation in the afternoon and evening and often canceling out over 24 hours[5,17]. Similar patterns are true for heat storage in canopies and air. For example, storage of latent energy in air can follow a diurnal pattern where energy storage increases during the day and energy is released when nighttime temperatures drop and condensation (dew) forms. We tested for average closure at longer time scales (e.g. weeks to months), with similar results to average daily closure at most sites. After daily averaging of SEB components, we performed visual quality control checks for each EC station's SEB data, removing periods of data that had clear data quality issues such as spikes, trends, and other systematic errors. Data periods that had poor closure, but no clear data problems were further investigated using the EC station micrometeorological data, gridded climate data and reference ET, visual inspection of site land cover and aerial imagery, and sometimes by simply asking site PIs for their insight. For example, some sites that were subject to high levels of smoke from nearby wildfires had suspect data records that were filtered out during those seasons. Other sites with suspected data quality issues were found to be in locations with complex terrain or too near to unrepresentative land cover which would cause invalidation of the assumptions of the EC technique, and these sites were removed from the selection of sites. Next, we further filtered out EC stations that had an average daily SEB closure error that exceeded 25% in the growing season and 40% during the non-growing season. Growing seasons start and end dates were determined using long-term climate data for each site[1]. Lastly, we applied the FLUXNET2015/ONEFlux method of correcting daily average latent energy flux (ET); this approach uses the energy balance ratio over moving windows (typically 15 days) to correct LE and H[23]. The FLUXNET2015/ONEFlux methods represent the most standardized approaches to processing EC data, and we think it is important to follow well established methods. Because the ONEFlux method uses the average energy balance ratio determined over moving windows, it does not force closure on a given date but results in a more conservative correction and may help account for energy imbalances that have longer timescales such as heat storage in wetland and riparian zones, or dense woody canopies[18]. One limitation of the energy balance ratio approach for SEB closure correction is that it assumes both LE and H are to be corrected by the same factor, i.e., that LE and H are both under- or over-estimated by equal proportions which is not always the case. There is some evidence based on data from the large sample EC dataset used in this study that LE and H both tend to be underestimated by similar proportions, with perhaps slightly more underestimation of LE than H on average for cropland sites[1]. Lastly, although not an active data processing step, the large number of flux sites used in this study (141) acts to dampen any systematic SEB error and biases that may be present in some sites or small samples of sites.

The screening and other procedures we used to limit SEB error in the flux data resulted in a dataset with less energy balance closure error than what is typically reported from large studies involving half-hourly fluxes. For example, we found a daily average closure error of 0.88 or 12% underestimation of LE + H, most other studies involving AmeriFlux data report closure error between 20–30%[10,11,24]. We acknowledge that the EC dataset still has SEB uncertainty and other errors that are difficult or currently impossible to account for, and that the ground data may thus have inherent limitations as a basis for RSET evaluation. Yet, this study possibly represents the most extensive assessment of RSET accuracy performed to date and the EC dataset used for comparison provides a consistent, reproducible benchmark for evaluation of the RSET data from all individual models. While the results are subject to revision in response to future improvements in characterization of ground data uncertainty, they should offer useful insight to absolute accuracies as well as relative performance across models and land cover types.

Supplementary Table 2. Daily statistical metrics for OpenET[6] models compared against paired closed flux tower daily ET[1,2] for sites grouped by their general land cover type. Data pairing was limited to days of satellite overpass (every 8 days in the case of Landsat, assuming clear-sky conditions). Slope is calculated as the linear regression slope forced through the origin. Measures of mean-bias-error (MBE), mean-absolute-error (MAE), and root-mean-square-error (RMSE) include the error in mm day^{-1} and normalized as a percentage of the weighted mean closed flux tower ET. Daily results for SIMS exclude soil evaporation from precipitation, which has been recently added to the SIMS model but was not included in the daily data from SIMS used in this analysis.

Land cover type	Statistic	Ensemble	DisALEXI	eeMETRIC	geeSEBAL	PT-JPL	SIMS	SSEBop	N sites	N data points
Croplands Mean station ET = 3.5 (mm/day)	Slope	0.86	0.87	0.92	0.8	0.85	0.85	0.93	60	5255
	MBE (mm)	-0.35 (-10.0%)	-0.31 (-8.8%)	-0.11 (-3.1%)	-0.57 (-16.2%)	-0.21 (-6.0%)	-0.41 (-11.7%)	-0.26 (-7.4%)	52	5225
	MAE (mm)	0.83 (23.6%)	0.96 (27.4%)	1.04 (29.6%)	1.14 (32.5%)	0.96 (27.4%)	0.9 (25.6%)	1.03 (29.3%)	52	5225
	RMSE (mm)	1.09 (31.1%)	1.26 (35.9%)	1.35 (38.5%)	1.47 (41.9%)	1.25 (35.6%)	1.2 (34.2%)	1.32 (37.6%)	52	5225
	R-squared	0.81	0.73	0.7	0.68	0.74	0.78	0.74	60	5255
Evergreen Forests Mean station ET = 2.3 (mm/day)	Slope	1.21	1.23	1.16	1.29	1.15	NA	1.19	17	1756
	MBE (mm)	0.73 (31.6%)	0.78 (33.8%)	0.54 (23.4%)	0.92 (39.8%)	0.77 (33.3%)	NA	0.69 (29.9%)	16	1754
	MAE (mm)	1.05 (45.5%)	1.23 (53.2%)	1.21 (52.4%)	1.33 (57.6%)	1.04 (45.0%)	NA	1.15 (49.8%)	16	1754
	RMSE (mm)	1.26 (54.5%)	1.48 (64.1%)	1.53 (66.2%)	1.63 (70.6%)	1.22 (52.8%)	NA	1.4 (60.6%)	16	1754
	R-squared	0.54	0.43	0.4	0.45	0.54	NA	0.42	17	1756
Grasslands Mean station ET = 1.7 (mm/day)	Slope	0.87	0.87	0.87	0.89	0.96	NA	0.78	27	3911
	MBE (mm)	-0.06 (-3.5%)	0.08 (4.7%)	-0.1 (-5.8%)	0.05 (2.9%)	0.19 (11.0%)	NA	-0.25 (-14.5%)	27	3911
	MAE (mm)	0.77 (44.8%)	0.9 (52.3%)	0.95 (55.2%)	1.19 (69.2%)	0.78 (45.3%)	NA	0.81 (47.1%)	27	3911
	RMSE (mm)	0.99 (57.6%)	1.13 (65.7%)	1.27 (73.8%)	1.57 (91.3%)	1.0 (58.1%)	NA	1.05 (61.0%)	27	3911
	R-squared	0.56	0.46	0.45	0.22	0.57	NA	0.53	27	3911
Mixed Forests Mean station ET = 2.2 (mm/day)	Slope	1.08	1.11	0.92	1.19	1.1	NA	1.08	14	1114
	MBE (mm)	0.48 (21.9%)	0.46 (21.0%)	-0.03 (-1.4%)	0.86 (39.3%)	0.74 (33.8%)	NA	0.45 (20.5%)	12	1105
	MAE (mm)	0.8 (36.5%)	0.84 (38.4%)	0.89 (40.6%)	1.19 (54.3%)	1.02 (46.6%)	NA	0.86 (39.3%)	12	1105
	RMSE (mm)	1.05 (47.9%)	1.11 (50.7%)	1.22 (55.7%)	1.52 (69.4%)	1.27 (58.0%)	NA	1.17 (53.4%)	12	1105
	R-squared	0.78	0.77	0.65	0.68	0.72	NA	0.71	14	1114
Shrublands Mean station ET = 1.2 (mm/day)	Slope	0.97	1	0.88	1.1	1.07	NA	0.81	26	3370
	MBE (mm)	0.05 (4.3%)	0.16 (13.8%)	-0.07 (-6.0%)	0.32 (27.6%)	0.3 (25.9%)	NA	-0.21 (-18.1%)	26	3370
	MAE (mm)	0.62 (53.4%)	0.72 (62.1%)	0.81 (69.8%)	0.99 (85.3%)	0.68 (58.6%)	NA	0.61 (52.6%)	26	3370
	RMSE (mm)	0.81 (69.8%)	0.92 (79.3%)	1.07 (92.2%)	1.31 (112.9%)	0.84 (72.4%)	NA	0.82 (70.7%)	26	3370
	R-squared	0.54	0.47	0.39	0.35	0.53	NA	0.56	26	3370
Wetlands Mean station ET = 3.2 (mm/day)	Slope	1.02	1.07	1.08	1.01	0.94	NA	0.97	9	1038
	MBE (mm)	0.32 (10.0%)	0.63 (19.7%)	0.47 (14.7%)	0.35 (11.0%)	0.14 (4.4%)	NA	0.09 (2.8%)	9	1038
	MAE (mm)	1.01 (31.7%)	1.18 (37.0%)	1.23 (38.6%)	1.3 (40.8%)	1.15 (36.1%)	NA	0.94 (29.5%)	9	1038
	RMSE (mm)	1.25 (39.2%)	1.44 (45.1%)	1.53 (48.0%)	1.64 (51.4%)	1.45 (45.5%)	NA	1.2 (37.6%)	9	1038
	R-squared	0.72	0.63	0.63	0.56	0.61	NA	0.73	9	1038

Supplementary Table 3. Monthly statistical metrics from comparisons between OpenET[6] models and closed flux tower monthly ET[1,2] for sites grouped by their general land cover type. Slope is calculated as the linear regression slope forced through the origin. Measures of mean-bias-error (MBE), mean-absolute-error (MAE), and root-mean-square-error (RMSE) include the error in mm month^{-1} and normalized as a percentage of the weighted mean closed flux tower ET.

Land cover type	Statistic	Ensemble	DisALEXI	eeMETRIC	geeSEBAL	PT-JPL	SIMS	SSEBop	N sites	N data points
Croplands Mean station ET = 91 (mm/month)	Slope	0.92	0.92	0.95	0.85	0.91	0.99	0.95	53	1652
	MBE (mm)	-5.27 (-5.8%)	-7.72 (-8.4%)	-2.44 (-2.7%)	-12.18 (-13.3%)	-2.9 (-3.2%)	4.32 (4.7%)	-6.08 (-6.7%)	44	1638
	MAE (mm)	15.84 (17.3%)	19.91 (21.8%)	21.23 (23.2%)	22.69 (24.8%)	18.12 (19.8%)	17.93 (19.6%)	22.4 (24.5%)	44	1638
	RMSE (mm)	20.44 (22.4%)	25.35 (27.7%)	26.97 (29.5%)	29.05 (31.8%)	23.67 (25.9%)	23.1 (25.3%)	27.72 (30.3%)	44	1638
	R-squared	0.9	0.86	0.83	0.83	0.87	0.86	0.85	53	1652
Evergreen Forests Mean station ET = 62 (mm/month)	Slope	1.24	1.3	1.17	1.34	1.17	NA	1.23	14	662
	MBE (mm)	16.8 (27.3%)	18.83 (30.6%)	10.78 (17.5%)	22.93 (37.3%)	16.22 (26.4%)	NA	16.71 (27.2%)	13	660
	MAE (mm)	24.68 (40.1%)	29.06 (47.2%)	25.94 (42.2%)	31.27 (50.8%)	25.11 (40.8%)	NA	26.84 (43.6%)	13	660
	RMSE (mm)	29.96 (48.7%)	34.75 (56.5%)	31.76 (51.6%)	38.2 (62.1%)	29.88 (48.6%)	NA	32.63 (53.0%)	13	660
	R-squared	0.62	0.55	0.55	0.59	0.58	NA	0.52	14	662
Grasslands Mean station ET = 40 (mm/month)	Slope	0.87	0.88	0.89	0.89	1.02	NA	0.78	18	626
	MBE (mm)	-0.88 (-2.2%)	2.4 (6.0%)	-1.77 (-4.4%)	2.96 (7.4%)	6.68 (16.7%)	NA	-6.2 (-15.5%)	18	626
	MAE (mm)	18.02 (45.1%)	20.33 (50.9%)	19.65 (49.2%)	27.15 (67.9%)	19.84 (49.6%)	NA	17.99 (45.0%)	18	626
	RMSE (mm)	22.72 (56.9%)	25.67 (64.2%)	25.21 (63.1%)	35.57 (89.0%)	24.22 (60.6%)	NA	22.45 (56.2%)	18	626
	R-squared	0.54	0.48	0.56	0.22	0.56	NA	0.53	18	626
Mixed Forests Mean station ET = 62 (mm/month)	Slope	1.19	1.14	1.06	1.3	1.2	NA	1.22	10	225
	MBE (mm)	17.72 (28.8%)	13.51 (21.9%)	6.55 (10.6%)	27.32 (44.4%)	22.35 (36.3%)	NA	18.93 (30.8%)	10	225
	MAE (mm)	19.76 (32.1%)	19.37 (31.5%)	18.55 (30.1%)	30.32 (49.3%)	23.79 (38.7%)	NA	22.03 (35.8%)	10	225
	RMSE (mm)	24.73 (40.2%)	24.12 (39.2%)	25.12 (40.8%)	36.0 (58.5%)	28.61 (46.5%)	NA	27.59 (44.8%)	10	225
	R-squared	0.87	0.85	0.79	0.81	0.85	NA	0.83	10	225
Shrublands Mean station ET = 31 (mm/month)	Slope	0.98	0.98	0.91	1.18	1.12	NA	0.78	24	656
	MBE (mm)	2.27 (7.4%)	2.64 (8.6%)	-1.84 (-6.0%)	11.38 (37.0%)	8.57 (27.9%)	NA	-6.17 (-20.1%)	24	656
	MAE (mm)	15.28 (49.7%)	16.84 (54.7%)	19.09 (62.0%)	22.07 (71.7%)	17.38 (56.5%)	NA	14.5 (47.1%)	24	656
	RMSE (mm)	19.27 (62.6%)	20.92 (68.0%)	23.64 (76.8%)	28.55 (92.8%)	20.8 (67.6%)	NA	17.98 (58.4%)	24	656
	R-squared	0.48	0.46	0.4	0.36	0.47	NA	0.57	24	656
Wetland/Riparian Mean station ET = 88 (mm/month)	Slope	1.06	1.14	1.11	1.06	0.99	NA	1.02	8	286
	MBE (mm)	11.9 (13.5%)	20.88 (23.7%)	14.52 (16.5%)	14.45 (16.4%)	8.84 (10.0%)	NA	5.29 (6.0%)	7	285
	MAE (mm)	25.94 (29.5%)	31.38 (35.7%)	31.75 (36.1%)	32.88 (37.4%)	28.69 (32.6%)	NA	21.61 (24.6%)	7	285
	RMSE (mm)	31.31 (35.6%)	37.85 (43.0%)	37.04 (42.1%)	41.01 (46.6%)	36.14 (41.1%)	NA	27.01 (30.7%)	7	285
	R-squared	0.75	0.69	0.68	0.61	0.65	NA	0.8	8	286

Supplementary Table 4. Growing season statistical metrics for OpenET[6] models against paired closed flux tower growing season ET[1,2] for sites grouped by their general land cover type. Growing seasons were defined based on long-term climate for each site, and monthly ET totals were used to aggregate to growing season periods[1]. Slope is calculated as the linear regression slope forced through the origin. Measures of mean-bias-error (MBE), mean-absolute-error (MAE), and root-mean-square-error (RMSE) include the error in mm season^{-1} and normalized as a percentage of the weighted mean closed flux tower ET.

Land cover type	Statistic	Ensemble	DisALEXI	eeMETRIC	geeSEBAL	PT-JPL	SIMS	SSEBop	N sites	N data points
Croplands Mean station ET = 605 (mm/growing season)	Slope	0.96	0.95	0.99	0.87	0.98	1.04	0.97	39	177
	MBE (mm)	-11.9 (-2.0%)	-22.34 (-3.7%)	7.72 (1.3%)	-67.04 (-11.1%)	3.12 (0.5%)	45.79 (7.6%)	-12.44 (-2.1%)	39	177
	MAE (mm)	78.14 (12.9%)	101.64 (16.8%)	93.58 (15.5%)	108.93 (18.0%)	94.03 (15.5%)	101.81 (16.8%)	103.85 (17.2%)	39	177
	RMSE (mm)	93.79 (15.5%)	112.64 (18.6%)	114.5 (18.9%)	123.54 (20.4%)	111.74 (18.5%)	125.07 (20.7%)	120.04 (19.8%)	39	177
	R-squared	0.87	0.84	0.82	0.83	0.83	0.79	0.82	39	177
Evergreen Forests Mean station ET = 217 (mm /growing season)	Slope	1.16	1.1	1.04	1.29	1.25	NA	1.1	14	94
	MBE (mm)	74.66 (34.4%)	64.76 (29.8%)	44.28 (20.4%)	112.74 (52.0%)	95.13 (43.8%)	NA	62.02 (28.6%)	14	94
	MAE (mm)	99.99 (46.1%)	105.34 (48.5%)	99.09 (45.7%)	129.68 (59.8%)	104.65 (48.2%)	NA	110.16 (50.8%)	14	94
	RMSE (mm)	117.11 (54.0%)	125.41 (57.8%)	119.38 (55.0%)	149.97 (69.1%)	125.63 (57.9%)	NA	127.47 (58.7%)	14	94
	R-squared	0.74	0.67	0.69	0.73	0.79	NA	0.67	14	94
Grasslands Mean station ET = 207 (mm/growing season)	Slope	1.06	1.05	1	1.19	1.33	NA	0.96	17	98
	MBE (mm)	8.05 (3.9%)	17.67 (8.5%)	-0.64 (-0.3%)	30.87 (14.9%)	47.56 (23.0%)	NA	-16.69 (-8.1%)	17	98
	MAE (mm)	78.68 (38.0%)	86.86 (42.0%)	82.16 (39.7%)	120.45 (58.2%)	92.37 (44.6%)	NA	74.65 (36.1%)	17	98
	RMSE (mm)	86.63 (41.9%)	98.91 (47.8%)	91.05 (44.0%)	135.22 (65.3%)	100.29 (48.4%)	NA	82.58 (39.9%)	17	98
	R-squared	0.55	0.51	0.51	0.36	0.59	NA	0.58	17	98
Mixed Forests Mean station ET = 265 (mm/growing season)	Slope	1.19	1.1	1.07	1.29	1.23	NA	1.24	10	45
	MBE (mm)	56.29 (21.2%)	36.74 (13.9%)	21.17 (8.0%)	87.03 (32.8%)	71.25 (26.9%)	NA	64.48 (24.3%)	10	45
	MAE (mm)	58.92 (22.2%)	46.27 (17.5%)	49.04 (18.5%)	89.85 (33.9%)	73.16 (27.6%)	NA	68.44 (25.8%)	10	45
	RMSE (mm)	69.02 (26.0%)	55.65 (21.0%)	60.69 (22.9%)	99.03 (37.4%)	79.33 (29.9%)	NA	84.78 (32.0%)	10	45
	R-squared	0.96	0.95	0.92	0.95	0.97	NA	0.93	10	45
Shrublands Mean station ET = 183 (mm/growing season)	Slope	1.1	1.06	1.08	1.32	1.27	NA	0.83	21	88
	MBE (mm)	10.84 (5.9%)	10.11 (5.5%)	-2.76 (-1.5%)	58.89 (32.2%)	42.8 (23.4%)	NA	-33.24 (-18.2%)	21	88
	MAE (mm)	73.09 (39.9%)	73.9 (40.4%)	95.41 (52.1%)	99.99 (54.6%)	83.49 (45.6%)	NA	65.16 (35.6%)	21	88
	RMSE (mm)	81.48 (44.5%)	84.35 (46.1%)	107.45 (58.7%)	113.11 (61.8%)	93.13 (50.9%)	NA	71.76 (39.2%)	21	88
	R-squared	0.5	0.48	0.47	0.47	0.46	NA	0.55	21	88
Wetlands Mean station ET = 500 (mm/growing season)	Slope	1.15	1.23	1.19	1.14	1.09	NA	1.08	8	39
	MBE (mm)	97.48 (19.5%)	150.59 (30.1%)	113.1 (22.6%)	110.08 (22.0%)	84.09 (16.8%)	NA	58.21 (11.6%)	8	39
	MAE (mm)	135.08 (27.0%)	167.16 (33.4%)	160.54 (32.1%)	155.88 (31.2%)	164.65 (32.9%)	NA	110.62 (22.1%)	8	39
	RMSE (mm)	159.49 (31.9%)	184.52 (36.9%)	181.02 (36.2%)	178.84 (35.8%)	194.73 (38.9%)	NA	132.09 (26.4%)	8	39
	R-squared	0.88	0.88	0.84	0.86	0.76	NA	0.89	8	39

Supplementary Table 5. Water year (October 1 through September 30) statistical metrics for OpenET[6] models against paired closed flux tower ET[1,2] for sites grouped by their general land cover type. Water year totals were aggregated from monthly ET data. Slope is calculated as the linear regression slope forced through the origin. Measures of mean-bias-error (MBE), mean-absolute-error (MAE), and root-mean-square-error (RMSE) include the error in mm year^{-1} and normalized as a percentage of the weighted mean closed flux tower ET.

Land cover type	Statistic	Ensemble	DisALEXI	eeMETRIC	geeSEBAL	PT-JPL	SIMS	SSEBop	N sites	N data points
Croplands Mean station ET = 991 (mm/water year)	Slope	0.91	0.91	0.93	0.83	0.96	1.01	0.91	16	72
	MBE (mm)	-73.91 (-7.5%)	-79.8 (-8.1%)	-56.15 (-5.7%)	-146.74 (-14.8%)	-27.98 (-2.8%)	28.07 (2.8%)	-84.74 (-8.6%)	16	72
	MAE (mm)	112.12 (11.3%)	151.46 (15.3%)	133.46 (13.5%)	175.98 (17.8%)	99.66 (10.1%)	120.47 (12.2%)	164.84 (16.6%)	16	72
	RMSE (mm)	121.87 (12.3%)	158.15 (16.0%)	145.12 (14.6%)	188.02 (19.0%)	107.12 (10.8%)	130.37 (13.2%)	176.24 (17.8%)	16	72
	R-squared	0.84	0.75	0.69	0.72	0.83	0.7	0.76	16	72
Evergreen Forests Mean station ET = 657 (mm/water year)	Slope	1.19	1.33	1.11	1.25	1.1	NA	1.18	3	6
	MBE (mm)	164.32 (25.0%)	259.4 (39.5%)	90.18 (13.7%)	226.86 (34.5%)	112.0 (17.0%)	NA	138.73 (21.1%)	3	6
	MAE (mm)	211.22 (32.1%)	326.4 (49.7%)	210.22 (32.0%)	226.86 (34.5%)	161.37 (24.6%)	NA	276.2 (42.0%)	3	6
	RMSE (mm)	221.08 (33.6%)	334.42 (50.9%)	216.12 (32.9%)	235.04 (35.8%)	166.33 (25.3%)	NA	284.57 (43.3%)	3	6
	R-squared	0.45	0.33	0.19	0.7	0.8	NA	0.15	3	6
Grasslands Mean station ET = 244 (mm/water year)	Slope	1.57	1.45	1.49	1.95	1.95	NA	1.42	2	15
	MBE (mm)	151.99 (62.3%)	119.58 (49.0%)	150.9 (61.8%)	286.78 (117.5%)	240.13 (98.4%)	NA	113.93 (46.7%)	2	15
	MAE (mm)	151.99 (62.3%)	122.8 (50.3%)	151.92 (62.3%)	286.78 (117.5%)	273.12 (111.9%)	NA	119.23 (48.9%)	2	15
	RMSE (mm)	163.81 (67.1%)	138.35 (56.7%)	167.65 (68.7%)	302.87 (124.1%)	274.15 (112.4%)	NA	139.15 (57.0%)	2	15
	R-squared	0.72	0.71	0.6	0.48	0.72	NA	0.59	2	15

Supplementary Table 6. Calendar year statistical metrics for OpenET[6] models against paired closed flux tower ET[1,2] for sites grouped by their general land cover type. Annual totals were aggregated from monthly ET data. Slope is calculated as the linear regression slope forced through the origin. Measures of mean-bias-error (MBE), mean-absolute-error (MAE), and root-mean-square-error (RMSE) include the error in mm year^{-1} and normalized as a percentage of the weighted mean closed flux tower ET.

Land cover type	Statistic	Ensemble	DisALEXI	eeMETRIC	geeSEBAL	PT-JPL	SIMS	SSEBop	N sites	N data points
Croplands Mean station ET = 973 (mm/calendar year)	Slope	0.93	0.93	0.95	0.84	0.98	1.05	0.92	14	69
	MBE (mm)	-49.17 (-5.1%)	-49.36 (-5.1%)	-34.85 (-3.6%)	-135.77 (-14.0%)	-5.65 (-0.6%)	73.58 (7.6%)	-59.93 (-6.2%)	14	69
	MAE (mm)	108.8 (11.2%)	141.49 (14.5%)	136.39 (14.0%)	178.99 (18.4%)	100.45 (10.3%)	149.31 (15.3%)	141.89 (14.6%)	14	69
	RMSE (mm)	122.41 (12.6%)	150.13 (15.4%)	154.24 (15.9%)	196.05 (20.1%)	111.33 (11.4%)	164.26 (16.9%)	156.75 (16.1%)	14	69
	R-squared	0.78	0.7	0.64	0.65	0.8	0.56	0.72	14	69
Evergreen Forests Mean station ET = 651 (mm/calendar year)	Slope	1.14	1.24	1.06	1.22	1.08	NA	1.1	4	7
	MBE (mm)	100.81 (15.5%)	155.37 (23.9%)	18.42 (2.8%)	197.79 (30.4%)	104.39 (16.0%)	NA	54.7 (8.4%)	4	7
	MAE (mm)	176.29 (27.1%)	300.17 (46.1%)	202.35 (31.1%)	197.79 (30.4%)	152.28 (23.4%)	NA	245.66 (37.7%)	4	7
	RMSE (mm)	182.83 (28.1%)	305.62 (46.9%)	206.68 (31.7%)	203.99 (31.3%)	157.7 (24.2%)	NA	251.08 (38.6%)	4	7
	R-squared	0.54	0.04	0.36	0.8	0.76	NA	0.14	4	7
Grasslands Mean station ET = 245 (mm/calendar year)	Slope	1.56	1.44	1.45	1.97	2	NA	1.42	2	16
	MBE (mm)	149.97 (61.2%)	121.09 (49.4%)	103.82 (42.4%)	300.2 (122.5%)	248.91 (101.6%)	NA	116.79 (47.7%)	2	16
	MAE (mm)	149.97 (61.2%)	125.68 (51.3%)	127.53 (52.1%)	300.2 (122.5%)	279.51 (114.1%)	NA	123.28 (50.3%)	2	16
	RMSE (mm)	161.31 (65.8%)	139.25 (56.8%)	141.2 (57.6%)	316.52 (129.2%)	280.79 (114.6%)	NA	144.36 (58.9%)	2	16
	R-squared	0.69	0.63	0.73	0.38	0.73	NA	0.52	2	16

Supplementary Table 7. Least squares linear regression model results using all paired monthly ET data for OpenET[6] models and flux tower ET[1,2] grouped by general land cover types.

	Croplands n=1652		Shrublands n=656		Grasslands n=626		Evergreen Forests n=662		Mixed Forests n=225		Wetlands n=286	
	slope	intercept	slope	intercept	slope	intercept	slope	intercept	slope	intercept	slope	intercept
Ensemble	0.9	3.23	0.82	8.17	0.64	15.59	1.09	11.67	1.04	15.07	0.79	34.28
DisALEXI	0.91	1.29	0.82	7.96	0.64	16.89	1.11	14.77	1.07	7.48	0.8	42.23
eeMETRIC	0.92	4.1	0.8	5.63	0.73	11.02	1.07	7.75	0.98	8.25	0.82	36.23
geeSEBAL	0.84	2.13	0.88	14.77	0.5	26.67	1.23	8.26	1.1	20.44	0.73	40.56
PT-JPL	0.81	12.49	0.83	15.12	0.7	22.44	1.03	10.77	0.97	24.37	0.64	43.69
SIMS	0.88	14.79	NA	NA	NA	NA	NA	NA	NA	NA	NA	NA
SSEBop	0.99	-6.25	0.76	1.42	0.63	10.39	0.94	22.45	1.06	16.05	0.85	21.19

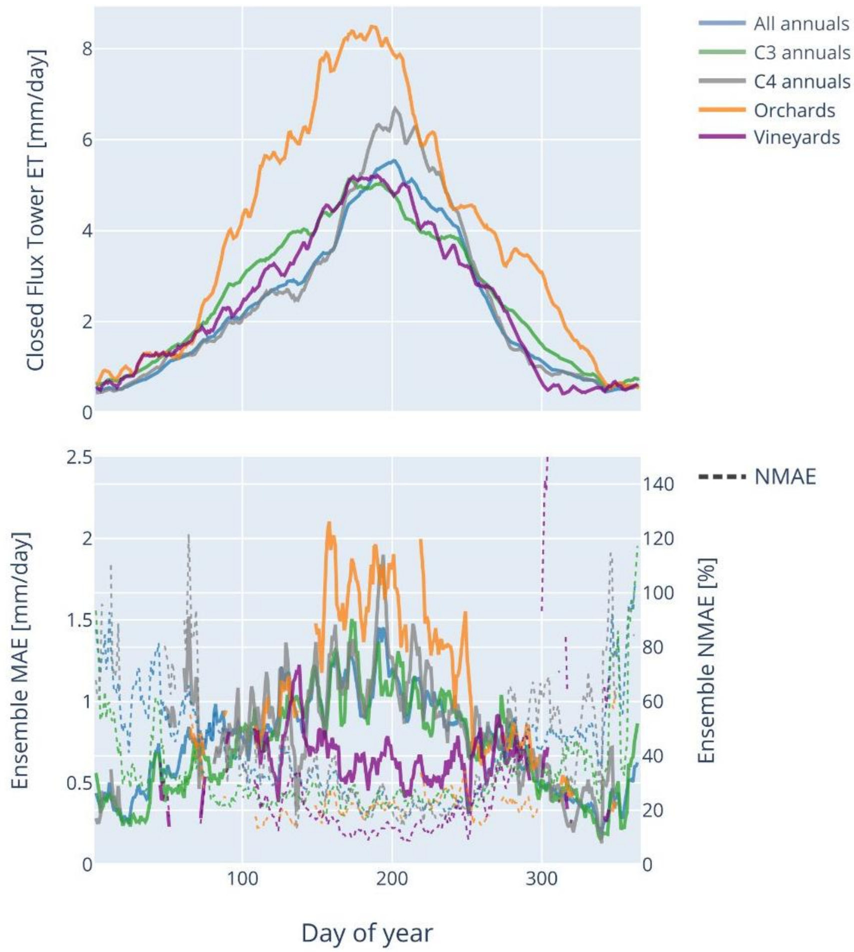

Supplementary Figure 1. Date of overpass OpenET[6] ensemble mean ET, mean-absolute-error (MAE), and MAE normalized by the mean closed flux tower ET[1,2] (NMAE) for each day of year using all paired model-measured data for cropland stations grouped by crop types. The NMAE data were smoothed using a 7-day moving average. Annual crops that had a mixed history of rotation between C3 and C4 crop types, e.g., corn-soy rotations, were not included in C3 or C4 results but were included in the combined (all annuals) grouping. The relative error rates for most cropland sites were typically below 25% of the mean closed flux tower ET during growing season periods; however, the low actual ET rates amplify the relative error during the colder periods of the year.

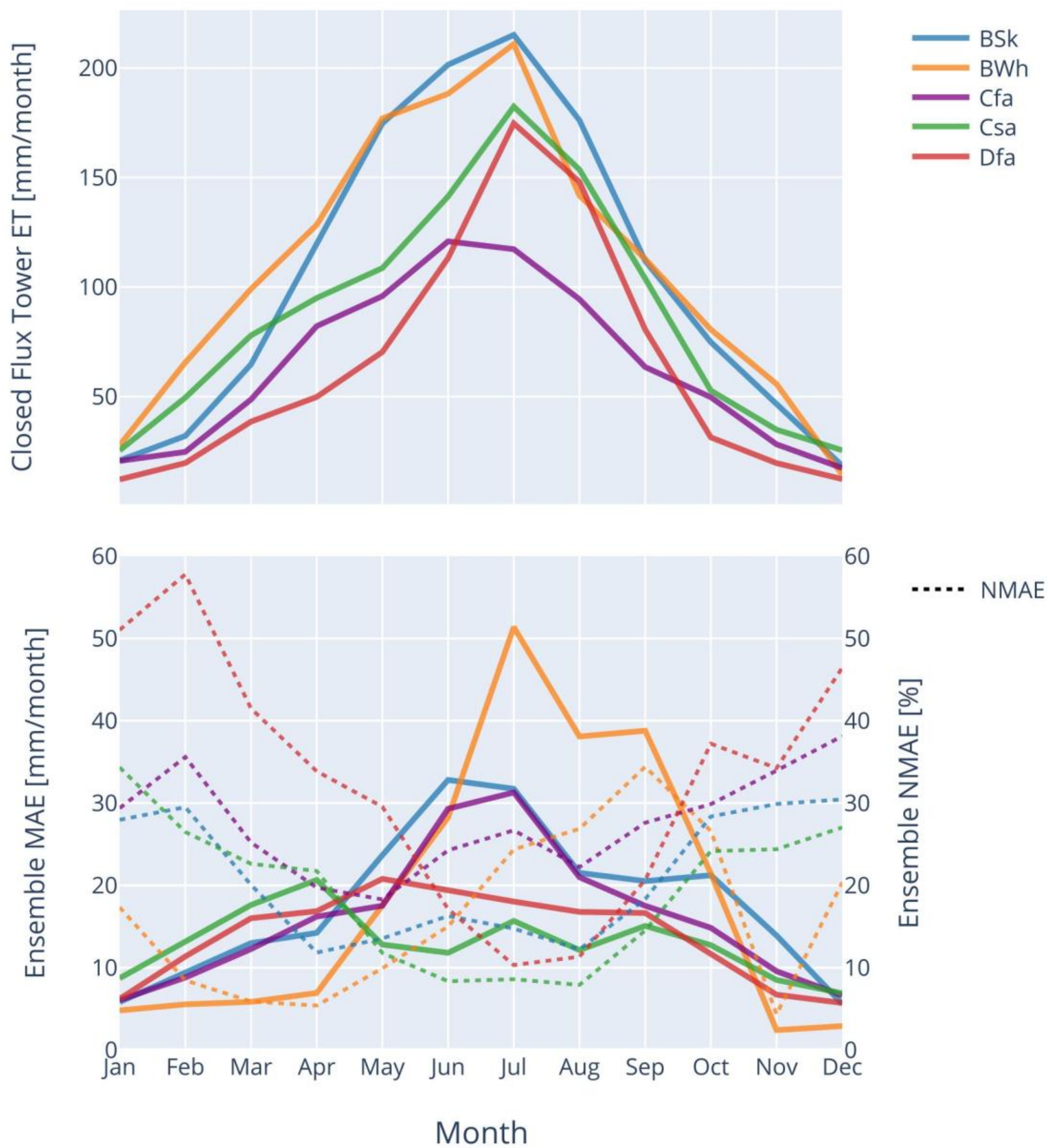

Closed Flux Tower ET [mm/month]
BSk
BWh
Cfa
Csa
Dfa
Ensemble MAE [mm/month]
Ensemble NMAE [%]
NMAE
Jan
Feb
Mar
Apr
May
Jun
Jul
Aug
Sep
Oct
Nov
Dec
Month

Supplementary Figure 2. Monthly OpenET[6] ensemble mean ET, mean-absolute-error (MAE), and MAE normalized by the mean closed flux tower ET[1,2] (NMAE) for each month using all paired model-measured data for all cropland stations grouped by their Köppen-Geiger climate classifications[25]. Climate zone abbreviations are defined as follows: cold and hot semi-arid steppe (Bsk + Bsh); hot and cold desert (Bwh + Bwk); humid subtropical (Cfa); hot- and warm-summer Mediterranean (Csa + Csb); and hot- and warm-summer humid continental (Dfa + Dfb). Relative errors are low for most climate zones during the summer months, typically below 15% of the mean closed flux tower ET. A different pattern is shown for desert cropland sites, with low relative error in the late winter and early spring, this may partially coincide with those sites' early growing season start. Similarly to non-growing periods for all crop types, relative error in croplands in humid regions is higher and this may be partially due to the lower ET rates in these regions.

Supplementary Table 8. Post-hoc Tukey test results for comparison of cropland monthly mean ET estimates from paired data (using 1,652 months from 53 stations) from each OpenET[6] model, the ensemble mean, and the unclosed and closed flux tower ET[1,2]. The upper and lower columns refer to the bounds on the 95% confidence interval for the difference between means for each group, and the null hypothesis of the test is that there is no significant difference between groups. Results suggest that the monthly mean ET for the OpenET ensemble value, PT-JPL, SIMS, and eeMETRIC are no different than the mean closed flux tower ET. Alternatively, DisALEXI, SSEBop, and geeSEBAL's monthly mean ET is statistically different from the closed flux tower ET, and their values are lower than the closed flux tower ET. Alternatively, the monthly mean unclosed flux tower ET was no different than the monthly means of DisALEXI, the ensemble value, geeSEBAL, and SSEBop, whereas eeMETRIC, SIMS, and PT-JPL had monthly mean ET values that were statistically different (higher) than the unclosed values.

group1	group2	meandiff	p-adj	lower	upper	reject
Closed	DisALEXI	-6.9776	0.0327	-13.6564	-0.2988	TRUE
Closed	Ensemble	-5.7191	0.1639	-12.3979	0.9596	FALSE
Closed	PT-JPL	-3.3806	0.7978	-10.0594	3.2982	FALSE
Closed	SIMS	4.567	0.4611	-2.1118	11.2458	FALSE
Closed	SSEBop	-7.2016	0.0234	-13.8803	-0.5228	TRUE
Closed	Unclosed	-12.0498	0.001	-18.7286	-5.371	TRUE
Closed	eeMETRIC	-3.0847	0.8812	-9.7635	3.5941	FALSE
Closed	geeSEBAL	-11.7724	0.001	-18.4512	-5.0937	TRUE
DisALEXI	Ensemble	1.2585	0.9	-5.4203	7.9372	FALSE
DisALEXI	PT-JPL	3.597	0.7368	-3.0818	10.2758	FALSE
DisALEXI	SIMS	11.5446	0.001	4.8658	18.2234	TRUE
DisALEXI	SSEBop	-0.224	0.9	-6.9027	6.4548	FALSE
DisALEXI	Unclosed	-5.0722	0.3088	-11.751	1.6065	FALSE
DisALEXI	eeMETRIC	3.8929	0.6534	-2.7859	10.5717	FALSE
DisALEXI	geeSEBAL	-4.7948	0.3901	-11.4736	1.8839	FALSE
Ensemble	PT-JPL	2.3385	0.9	-4.3402	9.0173	FALSE
Ensemble	SIMS	10.2861	0.001	3.6074	16.9649	TRUE
Ensemble	SSEBop	-1.4824	0.9	-8.1612	5.1963	FALSE
Ensemble	Unclosed	-6.3307	0.0798	-13.0095	0.3481	FALSE
Ensemble	eeMETRIC	2.6344	0.9	-4.0443	9.3132	FALSE
Ensemble	geeSEBAL	-6.0533	0.1121	-12.7321	0.6255	FALSE
PT-JPL	SIMS	7.9476	0.0069	1.2688	14.6264	TRUE
PT-JPL	SSEBop	-3.821	0.6737	-10.4997	2.8578	FALSE
PT-JPL	Unclosed	-8.6692	0.0019	-15.348	-1.9904	TRUE
PT-JPL	eeMETRIC	0.2959	0.9	-6.3829	6.9747	FALSE
PT-JPL	geeSEBAL	-8.3918	0.0031	-15.0706	-1.7131	TRUE
SIMS	SSEBop	-11.7686	0.001	-18.4473	-5.0898	TRUE
SIMS	Unclosed	-16.6168	0.001	-23.2956	-9.9381	TRUE
SIMS	eeMETRIC	-7.6517	0.0114	-14.3305	-0.9729	TRUE
SIMS	geeSEBAL	-16.3394	0.001	-23.0182	-9.6607	TRUE
SSEBop	Unclosed	-4.8483	0.3736	-11.527	1.8305	FALSE
SSEBop	eeMETRIC	4.1169	0.5903	-2.5619	10.7956	FALSE
SSEBop	geeSEBAL	-4.5709	0.4599	-11.2496	2.1079	FALSE
Unclosed	eeMETRIC	8.9651	0.001	2.2863	15.6439	TRUE
Unclosed	geeSEBAL	0.2774	0.9	-6.4014	6.9562	FALSE
eeMETRIC	geeSEBAL	-8.6877	0.0018	-15.3665	-2.009	TRUE

Supplementary Table 9. Post-hoc Tukey test results for comparison of cropland growing season mean ET estimates from paired data (using 177 growing season totals from 39 stations) from each OpenET[6] model, the ensemble mean, and the unclosed and closed flux tower ET[1,2]. The upper and lower columns refer to the bounds on the 95% confidence interval for the difference between means for each group, and the null hypothesis of the test is that there is no significant difference between groups. At growing season aggregation periods no model's mean ET was statistically different from the mean closed or unclosed flux tower ET.

group1	group2	meandiff	p-adj	lower	upper	reject
Closed	DisALEXI	-22.6187	0.9	-125.4256	80.1881	FALSE
Closed	Ensemble	-13.9134	0.9	-116.7203	88.8934	FALSE
Closed	PT-JPL	-3.7124	0.9	-106.5193	99.0944	FALSE
Closed	SIMS	51.0147	0.8151	-51.7922	153.8215	FALSE
Closed	SSEBop	-16.7235	0.9	-119.5304	86.0834	FALSE
Closed	Unclosed	-87.2393	0.1729	-190.0462	15.5676	FALSE
Closed	eeMETRIC	11.3371	0.9	-91.4698	114.1439	FALSE
Closed	geeSEBAL	-67.3389	0.5164	-170.1457	35.468	FALSE
DisALEXI	Ensemble	8.7053	0.9	-94.1015	111.5122	FALSE
DisALEXI	PT-JPL	18.9063	0.9	-83.9006	121.7132	FALSE
DisALEXI	SIMS	73.6334	0.3923	-29.1734	176.4403	FALSE
DisALEXI	SSEBop	5.8953	0.9	-96.9116	108.7021	FALSE
DisALEXI	Unclosed	-64.6205	0.5661	-167.4274	38.1863	FALSE
DisALEXI	eeMETRIC	33.9558	0.9	-68.8511	136.7627	FALSE
DisALEXI	geeSEBAL	-44.7201	0.9	-147.527	58.0867	FALSE
Ensemble	PT-JPL	10.201	0.9	-92.6059	113.0078	FALSE
Ensemble	SIMS	64.9281	0.5605	-37.8788	167.735	FALSE
Ensemble	SSEBop	-2.8101	0.9	-105.6169	99.9968	FALSE
Ensemble	Unclosed	-73.3259	0.3985	-176.1327	29.481	FALSE
Ensemble	eeMETRIC	25.2505	0.9	-77.5564	128.0573	FALSE
Ensemble	geeSEBAL	-53.4254	0.771	-156.2323	49.3814	FALSE
PT-JPL	SIMS	54.7271	0.7472	-48.0797	157.534	FALSE
PT-JPL	SSEBop	-13.0111	0.9	-115.8179	89.7958	FALSE
PT-JPL	Unclosed	-83.5269	0.2214	-186.3337	19.28	FALSE
PT-JPL	eeMETRIC	15.0495	0.9	-87.7574	117.8564	FALSE
PT-JPL	geeSEBAL	-63.6264	0.5843	-166.4333	39.1804	FALSE
SIMS	SSEBop	-67.7382	0.5091	-170.545	35.0687	FALSE
SIMS	Unclosed	-138.254	0.001	-241.0608	-35.4471	TRUE
SIMS	eeMETRIC	-39.6776	0.9	-142.4845	63.1292	FALSE
SIMS	geeSEBAL	-118.3535	0.0108	-221.1604	-15.5467	TRUE
SSEBop	Unclosed	-70.5158	0.4554	-173.3227	32.2911	FALSE
SSEBop	eeMETRIC	28.0606	0.9	-74.7463	130.8674	FALSE
SSEBop	geeSEBAL	-50.6154	0.8224	-153.4222	52.1915	FALSE
Unclosed	eeMETRIC	98.5763	0.0725	-4.2305	201.3832	FALSE
Unclosed	geeSEBAL	19.9004	0.9	-82.9064	122.7073	FALSE
eeMETRIC	geeSEBAL	-78.6759	0.2975	-181.4828	24.1309	FALSE

Supplementary Discussion 2. Ensemble outlier removal and spatial inter-model variability

Sophisticated, skill-based methods exist for integrating multiple RSET models and other data to improve RSET accuracy; however, they often employ data- and computationally-intensive approaches such as stochastic Bayesian averaging and other machine learning methods[26,27]. These methods can be difficult to communicate to stakeholders, and are prone to overfitting. Simple ensemble methods like the arithmetic mean may provide similar levels of accuracy[28] while offering a variety of advantages. In terms of accuracy at the flux sites, the simple mean after removal of outliers using the MAD approach gave comparable results to the simple arithmetic mean, the median, and standard deviation outlier removal approaches (Supplementary Table 10).

To characterize the spatial occurrence of outliers and to illustrate inter-model variability, we mapped the mean growing season (April through October) ET for each model and the ensemble with and without outlier removal, using the full OpenET domain over the period 2016–2022 (Extended Data Fig.'s 7–8 and Supplementary Figures 3–9). We found minor differences between the ensemble mean with and without outlier removal at most cropland pixels; however, outlier removal provides a layer of confidence in regions with sparse ground measurements where we know little about individual model biases[6].

In cropland pixels, the simple mean tended to be slightly higher than the MAD ensemble, indicating that, more often than not, a high estimate was discarded. However, the difference between the two methods rarely exceeded 10% of the mean growing season ET as calculated by the MAD approach (Supplementary Figure 3). In intensive agricultural regions, such as the California Central Valley and large fractions of the Central Plains, typically only a single or no model was identified as an outlier during growing season months (Extended Data Fig. 7). SIMS was deemed an outlier more often than other models in cropland pixels at a 20% frequency for growing season months, whereas the other models were deemed outliers at 8–10% frequency (Supplementary Table 11). Each model showed distinct spatial patterns in their divergence from the ensemble (Extended Data Fig. 8). Some of the substantial model biases we observe at the flux stations also show up in most cropland pixels over the growing season average, albeit with regional variations and exceptions. For example, the high relative bias of SIMS and low bias of geeSEBAL are most clearly pronounced in continental regions of the Central Plains and Midwest.

Supplementary Table 10. Monthly statistical metrics for several OpenET[6] ensemble approaches against closed flux ET[1,2] grouped by general land cover types. The 2xMADe, 2.5xMADe, and 3xMADe columns represent the ensemble approach where outlier model values are removed from the ensemble if they are outside of the band defined by the median absolute deviation (MAD), which is also adjusted by a coefficient. After removal of up to two models, defined by the MAD band, the ensemble mean is taken on a per-pixel basis to form the ensemble. The ensemble method adopted by OpenET was the 2MADe approach. See the Methods section of the article for a full description of the MAD approach. SAM represents the simple arithmetic mean without outlier removal; the STDEV columns use a per-pixel band defined by the sample standard deviation to identify outliers, much like the MAD approach. The “Throw 1” approach involves removing the furthest model from the mean and then computing the ensemble mean. “Throw 2” involves another iteration whereby the two models furthest from the mean will always be removed. To keep comparisons consistent, only one model was ever removed from any ensemble approach in non-agricultural locations because SIMS was not implemented in those instances.

Monthly ET Metrics for Different Ensemble Methods

Land Cover Type	Statistic	2xMADe	2.5xMADe	3xMADe	SAM	Median	1.5xSTDDEV	1.75xSTDDEV	Throw 1	Throw 2	N sites	N data points
Croplands Mean station ET = 91 (mm/month)	Slope	0.92	0.92	0.92	0.93	0.92	0.92	0.92	0.93	0.92	53	1652
	MBE (mm)	-5.27	-5.16	-5.07	-4.5	-5.06	-5.3	-4.91	-4.5	-5.31	44	1638
	MAE (mm)	15.84	15.8	15.73	15.31	15.74	15.94	15.6	15.31	16.08	44	1638
	RMSE (mm)	20.44	20.27	20.18	19.59	20.32	20.56	19.97	19.59	20.76	44	1638
	R-squared	0.9	0.9	0.9	0.91	0.9	0.9	0.9	0.91	0.9	53	1652
Evergreen Forests Mean station ET = 62 (mm/month)	Slope	1.24	1.24	1.24	1.24	1.24	1.24	1.24	1.24	1.23	14	662
	MBE (mm)	16.8	16.75	16.82	17.09	16.36	16.87	16.95	16.65	16.03	13	660
	MAE (mm)	24.68	24.44	24.31	24.02	24.9	24.49	24.05	25.1	25.93	13	660
	RMSE (mm)	29.96	29.65	29.53	28.9	30.2	29.72	28.94	30.45	31.52	13	660
	R-squared	0.62	0.63	0.63	0.65	0.61	0.63	0.64	0.61	0.59	14	662
Grasslands Mean station ET = 40 (mm/month)	Slope	0.87	0.87	0.88	0.89	0.87	0.87	0.89	0.86	0.86	18	626
	MBE (mm)	-0.88	-0.67	-0.27	0.81	-0.73	-0.64	0.7	-1.42	-1.8	18	626
	MAE (mm)	18.02	17.8	17.8	17.8	18.23	17.88	17.86	18.31	19.04	18	626
	RMSE (mm)	22.72	22.57	22.63	22.83	23.06	22.61	22.87	22.95	24.01	18	626
	R-squared	0.54	0.54	0.55	0.54	0.53	0.55	0.54	0.54	0.51	18	626
Mixed Forests Mean station ET = 62 (mm/month)	Slope	1.19	1.19	1.19	1.19	1.18	1.19	1.19	1.18	1.19	10	225
	MBE (mm)	17.72	17.6	17.9	17.73	17.23	17.99	17.86	17.32	17.44	10	225
	MAE (mm)	19.76	19.76	20.02	19.59	19.61	20.02	19.72	19.56	20.47	10	225
	RMSE (mm)	24.73	24.72	24.93	24.51	24.43	24.85	24.63	24.29	25.15	10	225
	R-squared	0.87	0.87	0.87	0.87	0.87	0.87	0.87	0.88	0.87	10	225
Shrublands Mean station ET = 31 (mm/month)	Slope	0.98	0.98	0.98	0.99	0.98	0.98	0.99	0.98	0.97	24	656
	MBE (mm)	2.27	2.29	2.31	2.92	2.41	2.26	2.84	1.98	1.43	24	656
	MAE (mm)	15.28	15.16	15.01	14.45	15.54	15.35	14.52	15.78	16.43	24	656
	RMSE (mm)	19.27	19.09	18.93	18.13	19.39	19.32	18.2	19.99	20.56	24	656
	R-squared	0.48	0.48	0.49	0.52	0.49	0.48	0.52	0.46	0.47	24	656
Wetland/ Riparian Mean station ET = 88 (mm/month)	Slope	1.06	1.06	1.06	1.06	1.06	1.06	1.06	1.06	1.06	8	286
	MBE (mm)	11.9	12.08	12.16	12.79	12.31	11.98	12.83	11.38	11.68	7	285
	MAE (mm)	25.94	25.81	25.78	25.79	25.61	25.96	25.95	25.64	25.38	7	285
	RMSE (mm)	31.31	31.02	30.78	30.63	30.89	31.21	30.87	31.06	31.47	7	285
	R-squared	0.75	0.76	0.76	0.77	0.76	0.76	0.76	0.75	0.75	8	286

Supplementary Table 11. Occurrence of models used in the OpenET[6] ensemble after the MAD outlier removal, as a percentage, using all monthly growing season data for all pixels that were classified as croplands for each year from 2016–2022, using all pixels in the current OpenET domain.

	DisALEXI	eeMETRIC	geeSEBAL	PT-JPL	SSEBop	SIMS
Annual All Lands	85.0	87.1	86.5	86.2	89.7	na
Growing Season All Lands	90.0	87.8	89.2	89.7	93.1	na
Annual Cropland	87.4	89.9	88.0	89.8	90.8	78.4
Growing Season Cropland	91.9	92.4	89.5	92.2	92.8	79.5

Supplementary Discussion 3. Potential use of OpenET data with regard to irrigation management

The scale of irrigated agriculture in terms of water use and costs is substantial, particularly in the western United States. Based on an assessment conducted in 2015, agricultural irrigation in the U.S. comprised an estimated 118,000 Mgal/day (446 million m3/day) of irrigation water withdrawals that were applied to about 63.5 million acres (25.7 million hectares); 81% of this water and 74% of the irrigated land was within the 17 most western states[29]. The majority of irrigation water, often over 70%, is "consumed" or lost to ET or plant tissue and not returned to the water reservoir from which it was withdrawn[29]. In 2018, total U.S. reported costs of off-farm water purchases was over $1.1 billion, pumping costs were about $2.5 billion, and other costs related to irrigation and technology maintenance were over $2 billion[30]. The cost structure of irrigation varies greatly by region, farm size, and irrigation type. Major expenses include the cost of water if purchased off site, pumping costs, and maintenance costs. Thus, while aggregate expenditures are substantial, potential cost savings resulting from use of ET data are difficult to generalize.

Environmental costs may be considered as well. For instance, most water (around 52%) used for irrigation in the U.S. comes from groundwater reservoirs[29]. High rates of groundwater withdrawal can result in lowered water tables due to extraction rates exceeding recharge, resulting in aquifer compaction land subsidence[31], aquifer contamination[32] and increased pumping costs. Withdrawals from both surface and groundwater thus deplete resource availability for environmental, municipal, and industrial uses.

The high economic and environmental costs of irrigation have resulted in incentives to reduce water consumption through irrigation strategies that may benefit from operational production of ET data. OpenET data can help irrigators manage applied irrigation water resources. For instance, daily data from the system might be used to guide ET-based irrigation scheduling operations[33,34] by estimating crop water consumption since the last wetting event. To calculate ET replacement, a conservative approach might involve summing ET and the associated average error for the crop type and time of year. Such use of an RSET framework for irrigation scheduling may or may not lead to water reductions in a given situation, depending on efficiency of prevailing irrigation practices on a given farm. Such efficiency is sensitive to both regional water availability and individual farm management strategies, which in turn are influenced by economic and social conditions as well as individual grower decisions reflecting risk aversion and overall familiarity with irrigation practices[35].

To directly quantify the benefits of readily accessible ET information through platforms such as OpenET, a project is underway that explores the economic and social benefits of adopting RSET for irrigation management in California[36]. The study focuses on almond orchards and wine grape vineyards, cropping systems where RSET model performance surpassed that of others examined in the study, suggesting greater adoption potential for irrigation management strategies. Water savings from RSET adoption will be quantified by comparing current irrigation management practices with a potential future state that utilizes RSET. Specifically, two approaches will be taken: the “cost savings to farmers,” determined by surface water prices and groundwater pumping costs, and a broader “economic value of water saved,” drawn from California’s water market data. These savings can offer direct economic benefit for growers, as well as broader social value in terms of sustained or expanded resources available for allocation to non-farm uses. This work aims to explore the value of RSET in almond and wine grape production and may possibly offer a template to evaluate benefits more widely across landscapes evaluated under the current study.

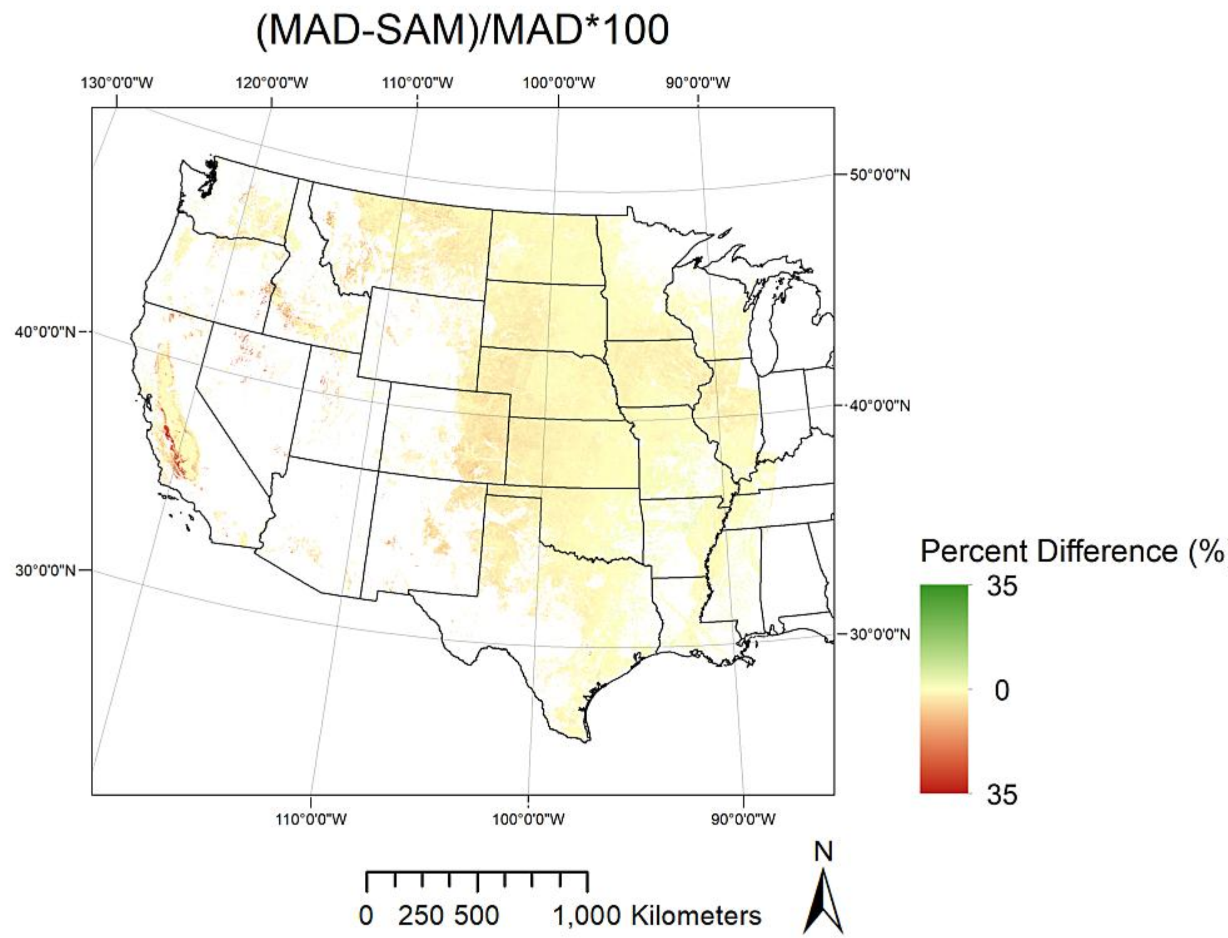

Supplementary Figure 3. Difference between mean growing season (April through October) OpenET[6] ensemble ET using the simple arithmetic mean (SAM) and the median absolute deviation (MAD) outlier removal ensemble mean as a percentage of the MAD growing season mean ET. Mean growing season ET values were calculated using monthly data from all pixels that were classified as croplands for each year from 2016–2022.

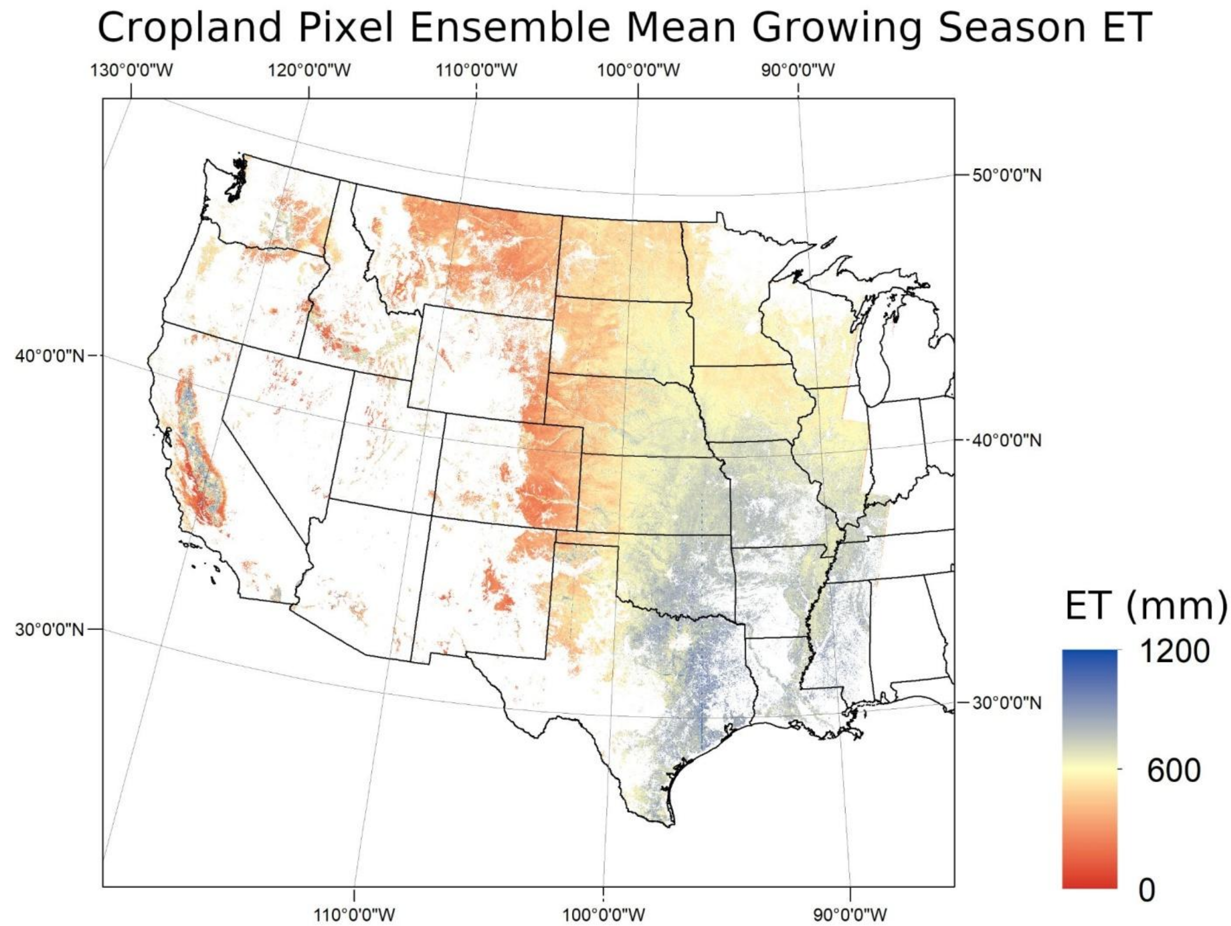

Supplementary Figure 4. The OpenET[6] ensemble mean growing season (April through October) ET for cropland pixels using the median absolute deviation (MAD) outlier removal ensemble approach. Monthly ET from 2016–2022 was used to build the map.

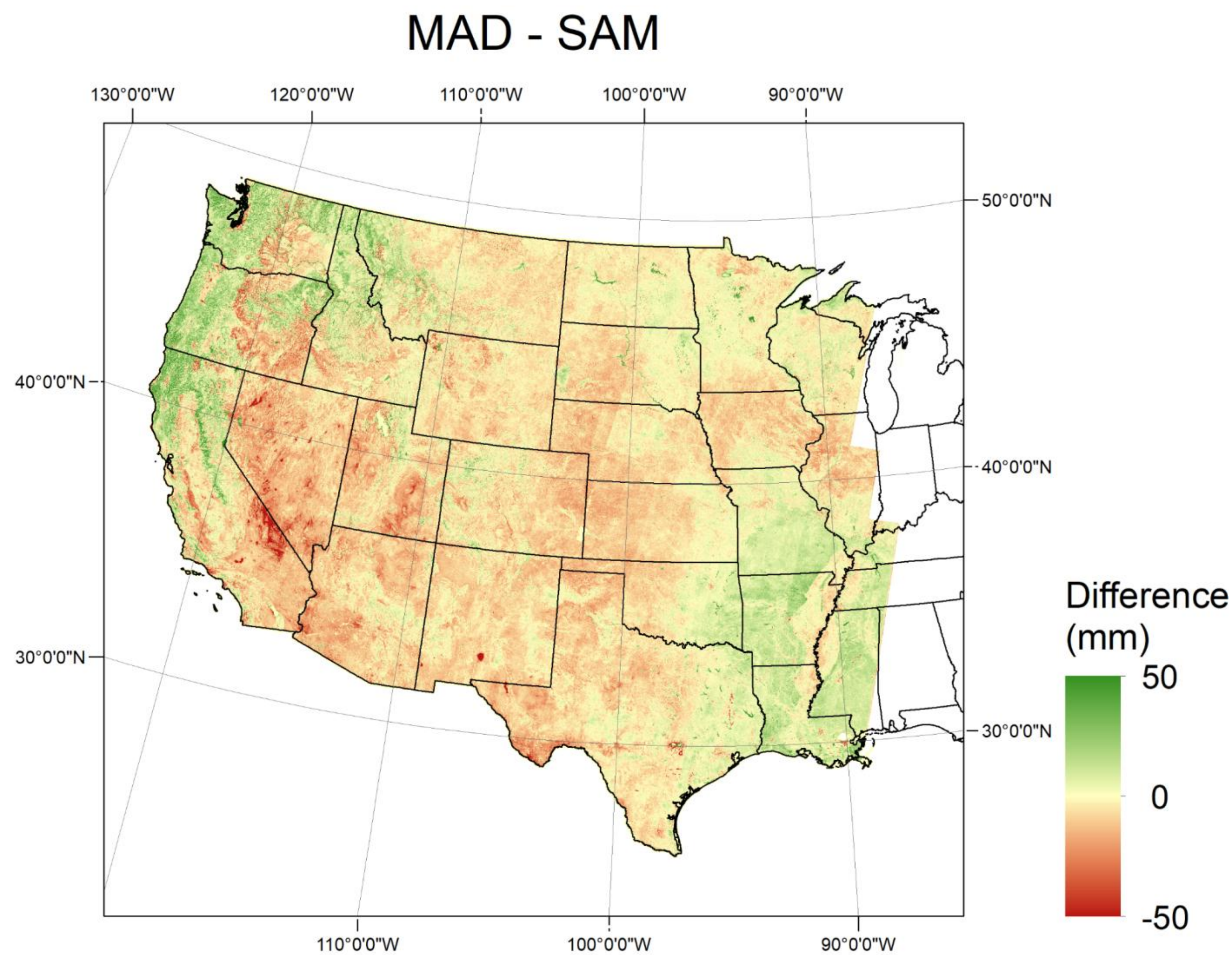

Supplementary Figure 5. The spatial differences between the OpenET[6] ensemble mean growing season (April through October) ET for all pixels using the median absolute deviation (MAD) outlier removal approach and the simple arithmetic mean (SAM). Monthly ET from 2016–2022 was used to build the map.

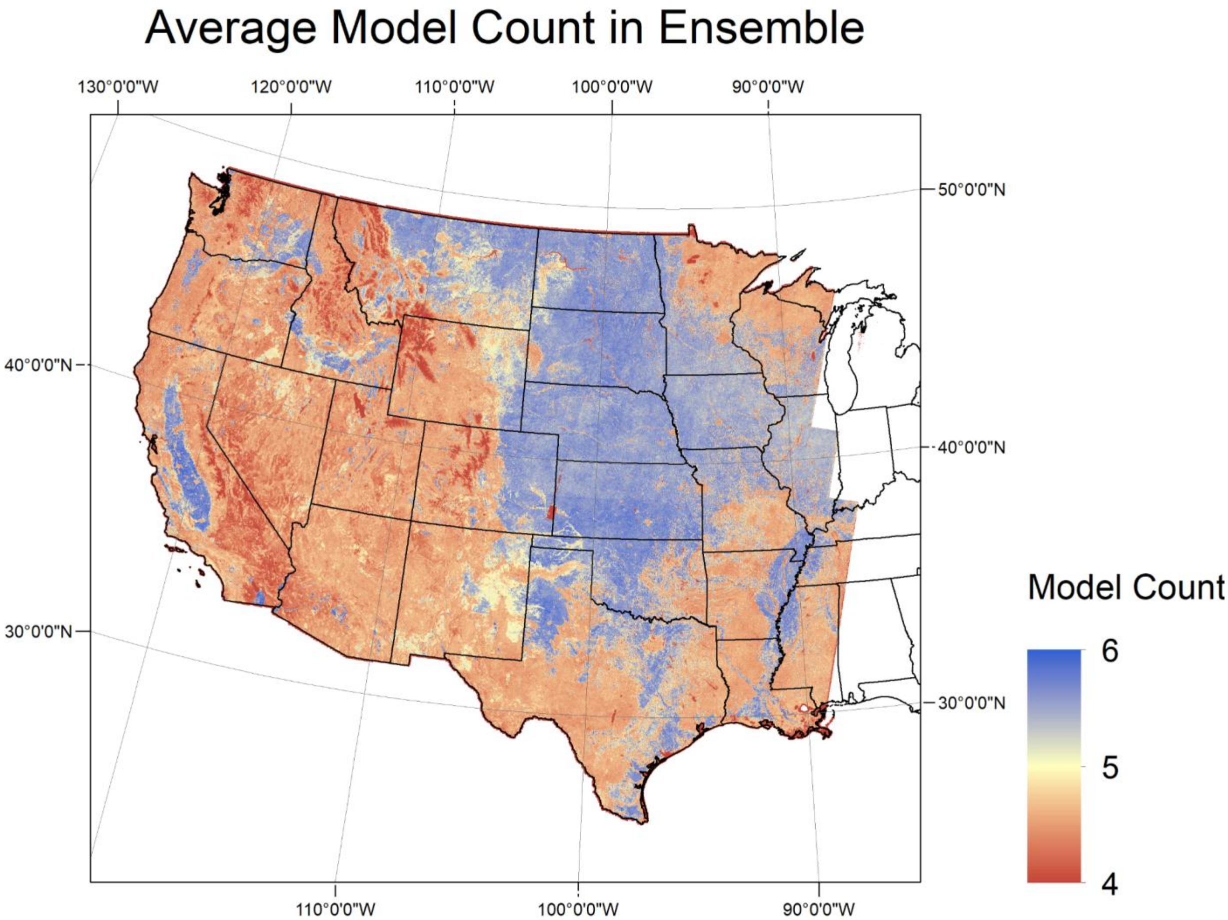

Supplementary Figure 6. The average count of models used in the OpenET[6] ensemble after median absolute deviation (MAD) outlier removal using all growing season monthly data from 2016–2022. A value of six indicates that no model was identified as an outlier, while four is the lower limit where a maximum of two models were removed as outliers before taking the ensemble mean.

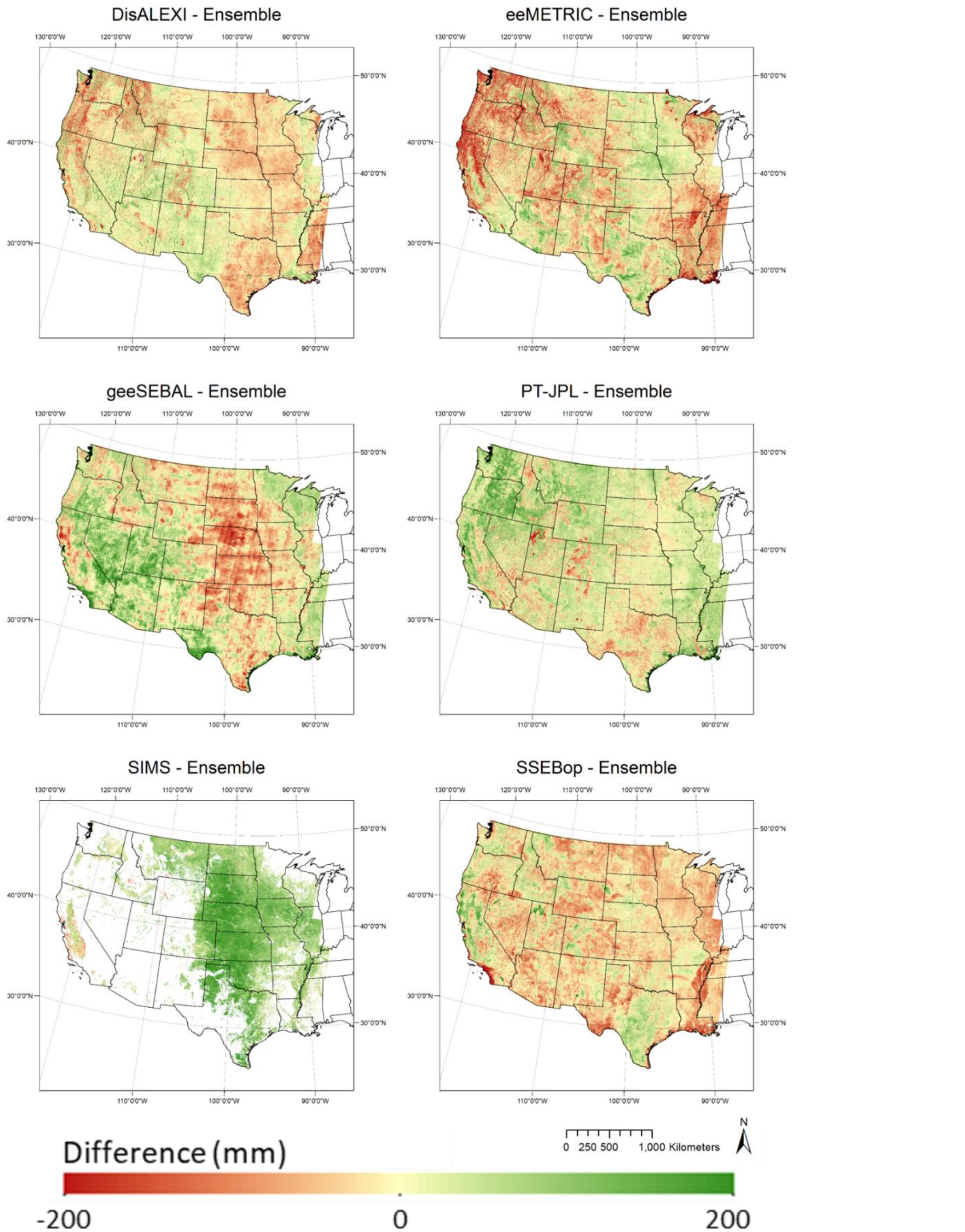

Supplementary Figure 7. Difference between mean growing season (April through October) ET from each OpenET[6] model minus the ensemble mean using all monthly data from all pixels for each year from 2016–2022. See Supplementary Discussion 3 for a discussion of the Landsat striping exhibited by geeSEBAL.

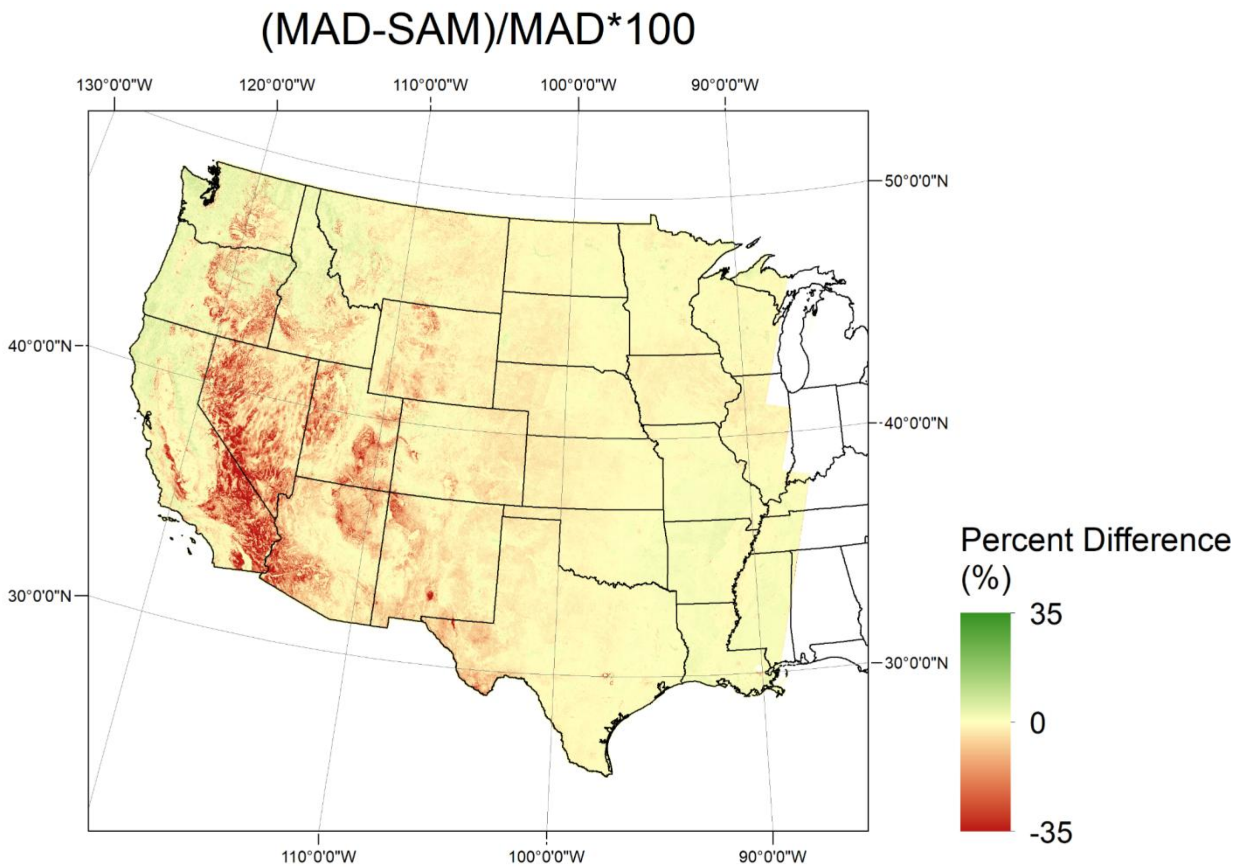

Supplementary Figure 8. Difference between mean growing season (April through October) OpenET[6] ET using the simple arithmetic mean (SAM) and the median absolute deviation (MAD) outlier removal ensemble mean as a percentage of the MAD growing season mean ET. Mean growing season ET values were calculated using monthly data from all pixels for each year from 2016–2022. Based on the long-term model differences from the ensemble (Supplementary Figure 5) it appears that geeSEBAL was frequently identified as an outlier in the western arid/semi-arid non-agricultural pixels, and it was typically estimating higher ET compared to the other models.

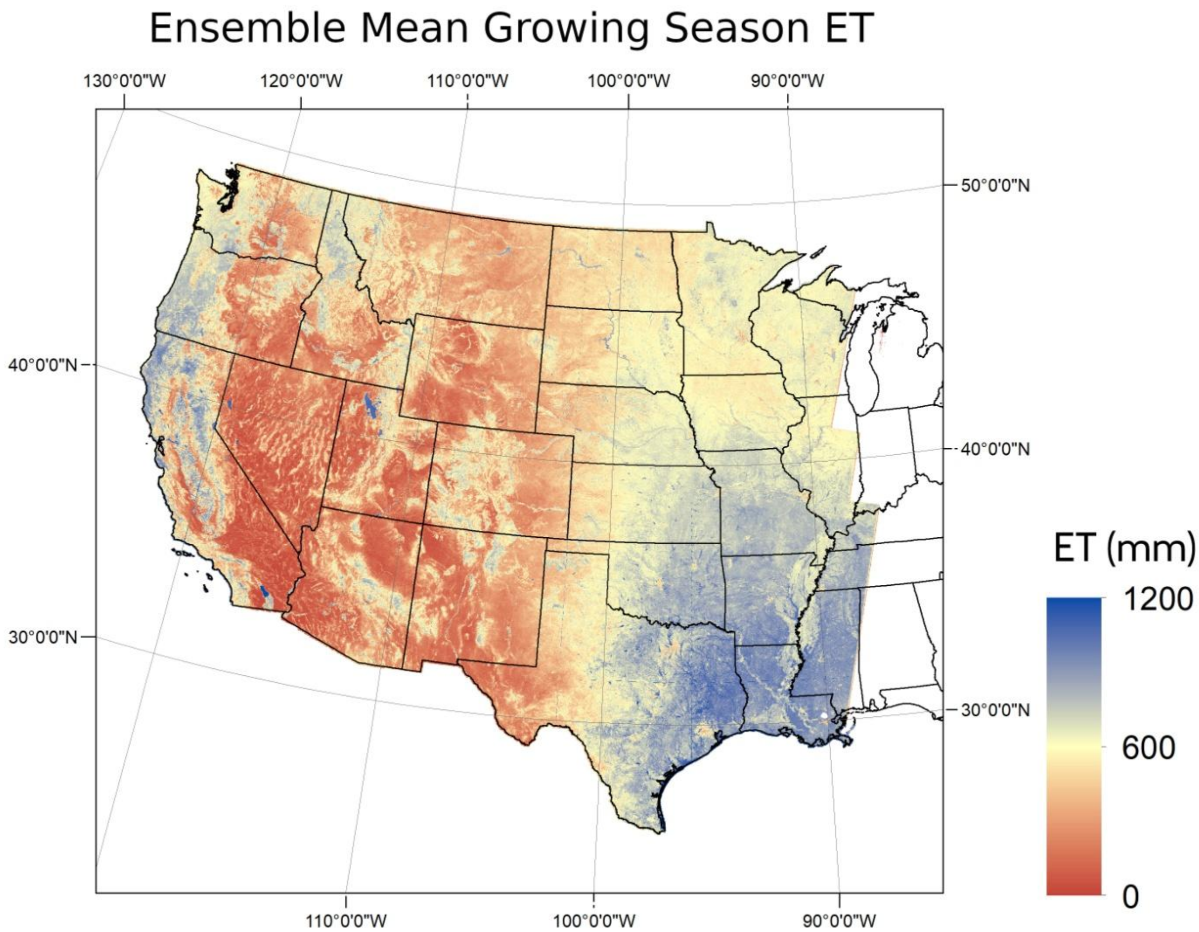

Supplementary Figure 9. The OpenET[6] ensemble mean growing season (April through October) ET for all pixels using the median absolute deviation (MAD) outlier removal ensemble approach. Monthly ET from 2016–2022 was used to build the map.

Supplementary Discussion 4. Landsat striping data artifact

Some of the surface energy balance (SEB) modeling approaches in the OpenET[6] ensemble are affected by environmental conditions related to the model domain area. For instance, geeSEBAL is a domain-dependent model, in which the results of ET estimates, in terms of distribution, amplitude and magnitude, depend on the domain area of the model. This domain area includes characteristics such as size area to select the endmembers, climate conditions, and land cover. Given the high sensitivity of geeSEBAL to the automated calibration process based on the hot and cold endmembers for internal calibration, the aforementioned domain characteristics impact the range of both cold and hot endmembers and consequently the ET estimates, making some Landsat striping visible especially over the Great Plains. A more comprehensive assessment of the domain-dependence of SEBAL is presented by Long et al.[37] and by Kayser et al.[38]. The

OpenET team members are currently conducting comprehensive research to reduce the domain-dependency and to improve the spatial accuracy of SEB models, especially for geeSEBAL. For further information regarding model known issues, readers are encouraged to visit the OpenET webpage.

Supplementary Table 12. Daily and monthly linear regression slope forced through the origin (Slope) and r^2 statistical metrics computed using the weighted approaches that were used by Melton et al.[6] to compare the OpenET ensemble against paired closed flux tower ET[1,2] for all cropland sites. These statistics are only provided for comparison with Melton et al.[6] because our calculation methods have since changed; specifically, in the current study, we did not employ weighting by the number of paired observations per site for these two statistics. Although this study incorporated over twice the number of stations and paired observations as Melton et al.[6], these statistical metrics were quite similar, with monthly ensemble values being within 0.01 from one another. When employing the weighting approaches previously used in Melton et al.[6] to compute the slope and r^2 statistics for the full datasets used in the current study, the daily ensemble r^2 improved from the previous study, from 0.84 to 0.87, and the daily Slope decreased from 0.90 to 0.87. Daily data pairing was limited to days of satellite overpass (every 8 days from in the case of Landsat, assuming clear-sky conditions). Daily results for SIMS exclude soil evaporation from precipitation, which has been recently added to the SIMS model but was not included in the daily data from SIMS used in this analysis.

Daily	Ensemble value	Range across individual models	N sites	N data points
sqrt(n) weighted mean Slope	0.87	0.81 to 0.92	52	5225
sqrt(n)/n weighted pooled r^2	0.87	0.77 to 0.84	52	5225

Monthly	Ensemble value	Range across individual models	N sites	N data points
sqrt(n) weighted mean Slope	0.94	0.87 to 1.04	44	1638
sqrt(n)/n weighted pooled r^2	0.95	0.89 to 0.94	44	1638

References

1. Volk, J. M. *et al.* Development of a benchmark Eddy flux evapotranspiration dataset for evaluation of satellite-driven evapotranspiration models over the CONUS. *Agric. For. Meteorol.* **331**, 109307 (2023).
2. Volk, J. M. *et al.* Post-processed data and graphical tools for a CONUS-wide eddy flux evapotranspiration dataset. *Data Brief* 109274 (2023).
3. Baldocchi, D. Measuring fluxes of trace gases and energy between ecosystems and the atmosphere--the state and future of the eddy covariance method. *Glob. Change Biol.* **20**, 3600–3609 (2014).
4. Chu, H. *et al.* Representativeness of Eddy-Covariance flux footprints for areas surrounding AmeriFlux sites. *Agric. For. Meteorol.* **301**, 108350 (2021).
5. Leuning, R., van Gorsel, E., Massman, W. J. & Isaac, P. R. Reflections on the surface energy imbalance problem. *Agric. For. Meteorol.* **156**, 65–74 (2012).
6. Melton, F. S. *et al.* OpenET: Filling a critical data gap in water management for the western United States. *JAWRA J. Am. Water Resour. Assoc.* **58**, 971–994 (2022).
7. Mauder, M., Foken, T. & Cuxart, J. Surface-energy-balance closure over land: a review. *Bound.-Layer Meteorol.* **177**, 395–426 (2020).
8. Moore, C. Frequency response corrections for eddy correlation systems. *Bound.-Layer Meteorol.* **37**, 17–35 (1986).
9. Wang, T., Verfaillie, J., Szutu, D. & Baldocchi, D. Handily measuring sensible and latent heat exchanges at a bargain: A test of the variance-Bowen ratio approach. *Agric. For. Meteorol.* **333**, 109399 (2023).

10. Wilson, K. *et al.* Energy balance closure at FLUXNET sites. *Agric. For. Meteorol.* **113**, 223–243 (2002).
11. Stoy, P. C. *et al.* A data-driven analysis of energy balance closure across FLUXNET research sites: The role of landscape scale heterogeneity. *Agric. For. Meteorol.* **171**, 137–152 (2013).
12. Stoy, P. C. *et al.* Separating the effects of climate and vegetation on evapotranspiration along a successional chronosequence in the southeastern US. *Glob. Change Biol.* **12**, 2115–2135 (2006).
13. Franssen, H. H., Stöckli, R., Lehner, I., Rotenberg, E. & Seneviratne, S. I. Energy balance closure of eddy-covariance data: A multisite analysis for European FLUXNET stations. *Agric. For. Meteorol.* **150**, 1553–1567 (2010).
14. Barr, A. G., Morgenstern, K., Black, T. A., McCaughey, J. H. & Nesic, Z. Surface energy balance closure by the eddy-covariance method above three boreal forest stands and implications for the measurement of the CO2 flux. *Agric. For. Meteorol.* **140**, 322–337 (2006).
15. Bambach, N. *et al.* Evapotranspiration uncertainty at micrometeorological scales: the impact of the eddy covariance energy imbalance and correction methods. *Irrig. Sci.* **40**, 445–461 (2022).
16. Foken, T. The energy balance closure problem: an overview. *Ecol. Appl. Publ. Ecol. Soc. Am.* **18**, 1351–1367 (2008).
17. Meyers, T. P. & Hollinger, S. E. An assessment of storage terms in the surface energy balance of maize and soybean. *Agric. For. Meteorol.* **125**, 105–115 (2004).
18. Meier, R., Davin, E. L., Swenson, S. C., Lawrence, D. M. & Schwaab, J. Biomass heat storage dampens diurnal temperature variations in forests. *Environ. Res. Lett.* **14**, 084026 (2019).

19. Montagnani, L. *et al.* Estimating the storage term in eddy covariance measurements: the ICOS methodology. *Int. Agrophysics* (2018).

20. Sauer, T. J. & Horton, R. Soil heat flux. *Micrometeorology Agric. Syst.* **47**, 131–154 (2005).

21. Brotzge, J. & Duchon, C. A field comparison among a domeless net radiometer, two four-component net radiometers, and a domed net radiometer. *J. Atmospheric Ocean. Technol.* **17**, 1569–1582 (2000).

22. Novick, K. A. *et al.* The AmeriFlux network: A coalition of the willing. *Agric. For. Meteorol.* **249**, 444–456 (2018).

23. Pastorello, G. *et al.* The FLUXNET2015 dataset and the ONEFlux processing pipeline for eddy covariance data. *Sci. Data* **7**, 1–27 (2020).

24. Eshonkulov, R. *et al.* Evaluating multi-year, multi-site data on the energy balance closure of eddy-covariance flux measurements at cropland sites in southwestern Germany. *Biogeosciences* **16**, 521–540 (2019).

25. Rubel, F., Brugger, K., Haslinger, K. & Auer, I. The climate of the European Alps: Shift of very high resolution Köppen-Geiger climate zones 1800–2100. *Meteorol. Z.* **26**, 115–125 (2017).

26. Shang, K. *et al.* DNN-MET: A deep neural networks method to integrate satellite-derived evapotranspiration products, eddy covariance observations and ancillary information. *Agric. For. Meteorol.* **308**, 108582 (2021).

27. Yao, Y. *et al.* Improving global terrestrial evapotranspiration estimation using support vector machine by integrating three process-based algorithms. *Agric. For. Meteorol.* **242**, 55–74 (2017).

28. Schwalm, C. R. *et al.* Toward “optimal” integration of terrestrial biosphere models. *Geophys. Res. Lett.* **42**, 4418–4428 (2015).

29. Dieter, C. A. *et al. Estimated use of water in the United States in 2015*. *Circular* 76 http://pubs.er.usgs.gov/publication/cir1441 (2018) doi:10.3133/cir1441.

30. USDA National Agricultural Statistics Service. 2017 Census of Agriculture.

31. Liu, Z. *et al.* Monitoring groundwater change in California's central valley using sentinel-1 and grace observations. *Geosciences* **9**, 436 (2019).

32. Jasechko, S. *et al.* Global aquifers dominated by fossil groundwaters but wells vulnerable to modern contamination. *Nat. Geosci.* **10**, 425–429 (2017).

33. Cahn, M. D. & Johnson, L. F. New approaches to irrigation scheduling of vegetables. *Horticulturae* **3**, 28 (2017).

34. Cahn, M., Smith, R. & Melton, F. Field evaluations of the CropManage decision support tool for improving irrigation and nutrient use of cool season vegetables in California. *Agric. Water Manag.* **287**, 108401 (2023).

35. Foster, T., Gonçalves, I. Z., Campos, I., Neale, C. & Brozović, N. Assessing landscape scale heterogeneity in irrigation water use with remote sensing and in situ monitoring. *Environ. Res. Lett.* **14**, 024004 (2019).

36. Nocco, M. A. *et al.* Exploring almond, water, and climate linkages with the Tree Remote sensing of Evapotranspiration eXperiment (T-REX). in vol. 2022 GC36B-05 (2022).

37. Long, D., Singh, V. P. & Li, Z. How sensitive is SEBAL to changes in input variables, domain size and satellite sensor? *J. Geophys. Res. Atmospheres* **116**, (2011).

38. Kayser, R. H. *et al.* Assessing geeSEBAL automated calibration and meteorological reanalysis uncertainties to estimate evapotranspiration in subtropical humid climates. *Agric. For. Meteorol.* **314**, 108775 (2022).